IOSR Journal of Applied Geology and Geophysics (IOSR-JAGG)
e-ISSN: 2321–0990, p-ISSN: 2321–0982.Volume 5, Issue 4 Ver. II (Jul. – Aug. 2017), PP 06-35
www.iosrjournals.org

Trace Including Ree+Y And Organic Geochemistry Of Kuşakdağı And Gökçepinar Formations In The Beyreli (Hadim-Konya) Area, Central Taurides, Southern Turkey: Implications For Source Rock Potential, Provenance, Paleo-Environment And Tectonic Setting

J. Kareem and Ş. Küpeli
Department of Geology, Selcuk University, 42031 Selçuklu, Konya, Turkey
Corresponding Author: J. Kareem and Ş. Küpeli

Abstract: *The investigation area comprised of Beyreli (Hadim-Konya) village and the surrounding area in the Central Taurus Belt, Southern Turkey. A total of forty-eight bulk samples from the Late Permian and Early Triassic Kuşakdağı (K) and Gökçepınar Formations (T) were analyzed to investigate the organic carbon contents, types, maturities, hydrocarbon potentials of the Kuşakdağı Formation and tectonic settings, provenance and depositional conditions of both Formations by using geochemical data. The Formations are represented by limestone and bituminous shale units. Geochemical data such as TOC content, Tmax and HI values from Rock-Eval pyrolysis analysis show that the Kuşakdağı formation does not contain significant amounts of organic matter for the production of petroleum while is more suitable for the production of gas. However, some source-rock inter-levels in the Kuşakdağı Formation had TOC contents that are over 0.5% which is the proposed minimum limit value for petroleum parent rock. HI and Tmax indicate that most of the source rock samples from the Kuşakdağı Formation are over matured and their primary organic matter types are the Type III and Type IV kerogen (coaly). PAAS normalized REE values of the samples from the formations show that the slightly LREE enriched, more or less flat REE patterns (expressed as average* $(La/Yb)_{PN}$ *=1,34) associated with weakly positive Eu (average=1,01, n=28) and weakly negative Ce (average 0,90; n=28) anomalies. Trace and rare earth element (REE) geochemistry, discrimination diagrams and some elemental ratios show that the Kuşakdağı and Gökçepınar Formations have been deposited from mid to shallow saline seawater under the anoxic conditions on the continental island arc and partially oceanic island arc tectonic settings during the hot-dry climates. Terrigenous materials included in the Kuşakdağı and Gökçepınar formations were also derived from intermediate igneous rocks exposed on the provenance area.*

Keywords*: Beyreli (Hadim-Konya, Turkey), Rare Earth Element, Rock-Eval pyrolysis, Kerogen, Kuşakdağı and Gökçepınar Formations, Tectonic Setting, Total organic carbon (TOC).*

Date of Submission: 11-07-2017 Date of acceptance: 31-07-2017

I. Introduction

The study area is located approximately 110 km south of the province of middle Taurus (Konya) and it covers the Beyreli Village (Hadim-Konya) and its surroundings (Fig. 1). The study area extends from about longitudes 36°50'50.4"N and latitudes 32°22'38.7"E. The main purpose of the present study is to investigate organic geochemical and organo-petrographic characteristics of the Kuşakdağı Formation and examining hydrocarbon potentials to get knowledge about its source rock potential and whether if it can be a source rock or not. Its depositional environment, stage of maturity and potential for hydrocarbon generation were investigated. The outcrop samples of Kuşakdağı Formation were collected and analyzed by Rock-Eval VI pyrolysis. Rock–Eval pyrolysis is used routinely as a rapid screening method for examining the type, origin, and maturity of the OM of potential source rocks (Mrkić et al., 2011). A total of 20 samples were analyzed by Rock–Eval pyrolysis. Petroleum generation from source rocks is determined by the abundance and type of organic matter present and its thermal maturation (Alizadeh et al., 2012). In addition, it was aimed to determine the rare earth element (NTE) contents, major-trace and environmental properties of bituminous shale and carbonate limestone rocks of the Late Permian Kuşakdağı and Lower Triassic Gökçepınar Formations. Our aims is to trace the depositional environment, to interpret the possible source of REEs. During the past few decades, the behavior and mode of distribution of rare earth elements (REEs) in carbonate rocks were extensively investigated by many researchers (Abedini and Calagari, 2015; Armstrong-Altrin et al., 2003; Chen et al., 2014; H. Elderfield et al., 1990; Ephraim, 2012; Hua et al., 2013; Kuşcu et al., 2016; J. Madhavaraju et al., 2010; J. Madhavaraju and Lee, 2009;

Nagarajan et al., 2011; Nothdurft et al., 2004; Oni et al., 2014; Singh et al., 2016; Tao et al., 2016; Tuchscherer et al., 2005). The studies done revealed that the important factors that affect the enrichment and depletion of REEs in carbonate rocks are 1) the relevance to domain of the source (Murray et al., 1991), 2) the variety in surface productivity (Toyoda et al., 1990), 3) the quantities of detrital materials of terrigenous source (Nagarajan et al., 2011), 4) biogenic sediments from seawater (Murray et al., 1991), 5) the variety in oxygen level of seawater (Liu et al., 1988), 6) the lithology and diagenesis (J. Madhavaraju and Ramasamy, 1999), and 7) scavenging processes related to salinity, depth, and oxygen level of seawater (Greaves et al, 1999). Rare earth element (REE) concentrations in former carbonate rocks are important to detect the marine and non-marine origins of REE (Banner et al., 1988; Frimmel, 2009; Zhao et al., 2009). Earlier studies showed that the carbonate rocks have low REE concentrations (Goldberg et al., 1963; M. A. Haskin and Haskin, 1966; Tlig and M'rabet, 1985), and the REE patterns in carbonate rocks are primarily affected by depositional environment (J. Madhavaraju and Ramasamy, 1999; Murray et al., 1992; Murray et al., 1990) and diagenetic processes (Armstrong-Altrin et al., 2003; Fu et al., 2011; Morad et al., 2010; Scherer and Seitz, 1980; Schieber, 1988). İn this study the bituminous shale and limestone rocks has been investigated in terms of total organic carbon, major, trace and rare earth element geochemistry.

II. Geological setting

The study area is located in the middle Taurus Mountains approximately 110 km south of the province of Konya, and it covers Beyerli Village and its surroundings (Fig. 2). Beyreli village lays about 17 km south of Hadim, 19 km to the Geyik Mountains, 17 km to Eğri Lake and 15 km to Tashkent. Beyerli Village (Hadim) region and its surroundings in Central Taurus Mountains was first discovered by (M. Blumenthal, 1944; M. M. Blumenthal, 1951), and his crew M. Blumenthal and Göksu (1949) at the regional scale. Allochthonous slices of the Taurus Mountains that belongs to Aladağ unit and have the age of the Middle Carboniferous to the Early Cretaceous take place around the beyreli village. These sequences are the highest alloktons of the Middle Taurus Mountains and are also known as the Gevne nape. The stratigraphic section of the Aladağ Unit around Beyreli area begins with Yarıcak Formation of gold-rich fuzulian, coralian, crinoid and brachiopod limestones and continuing upward with fossiliferous limestone-quartzite alternately. Early Permian aged Arpalık Formation comes in conformity above Yarıcak Formation. Abundant fuzulized and crinoid limestones with sandy carbonate intercalations lays at the top of Arpalık Formation wıth Girvenella algal Pizolites composed of Oncolytic carbonates beneath it, and it is eroded by the Late Permian Kuşakdağı Formation. The Kuşakdağı Formation begins with a quartzite at the bottom and continuing in the form of shale-quartzite intercalated, scarcely Foraminifera and abundant algal limestone and its conformity with the Early Triassic Gökçepınar Stromatolite Oolitic carbonate -bearing limestone. These shallow marine carbonates of Lower Triassic enter the Early-Middle Triassic Göztaşı Formation at the top with its shale and abundant bivalvic marl-clay limestones composition. The Göztaşı Formation is covered with Middle Triassic Beyreli Formation in the form of sandy-silty- clayey carbonate flysch sequences. During the Liassic-Dogger period a red colored, cross-bedded conglomerate-sandstone-mudstone with lignite content, terrestrial Çamiçi Formation was formed. A semi-terrestrial of Dogger-Malm aged with a mudstone-shale-clayey limestone containing very fine lignite and gypsum bands lay above the Çamiçi Formation named Dedebeleni Formation (Turan, 2010). The Kuşakdağı Formation, which is the thickest and widespread unit in the study area (Fig. 3), can be seen around the Yüremece Plateau, Tekesar Hill, Sarituzla, Karagöl Hill and Ayıpınarı Plateau. The lithology of the Formation is predominantly dark gray-black colored limestone, very dense algal and it has a bad smell due to its high organic matter content. The thickness of Kuşakdağı Formation, which is in conformity with the Early Triassic Gökçepinar limestone, was found to be 800 m in the measured stratigraphic section built along the Çamurluk valley-Kuşakdağı-Gökçepınar Plateau (Fig. 5). The lithological evolution of the Formation and the abundance of ***Mizzia*** **sp.,** and the ***Hemigordius*** **sp.,** and their different biotopes as seen in (Fig. 4), This, therefore, suggest that the sediments of the late Permian time probably occurred in the tidal sea environment, including the reef lagoon regions. Gökçepınar unit presents stratigraphic boundary relations in conformity with the Kuşakdağı Formation at the bottom and Göztaşı Formation from above and has the thickness of 80 m at the type section. According to the stratigraphic location of this Formation and the paleontological and stratigraphic investigations of earlier researchers (Göktepe and Güvenç, 1997; Kuşçu, 1983; Özgül, 1976, 1996), this Formation was given the Early Triassic age. The algal micritic facies of the Gökçepınar limestone unit, indicate that the unit had deposited under the wave floor in low energy zones. However, during the next periods, the rise in water energy brought about the removal of the carbonate mud from the environment and leads to forming Oolitic-Pizolitic facies in the marine basin of Early Triassic (Turan, 2010).

III. Samples and Analytical Procedures

In this study, 41 samples were collected from the Kuşakdağı Formation in order to detect geochemical data of the formation. A total of 20 samples were selected for Total Organic Carbon (TOC) and pyrolysis (Rock-Eval) analysis. The total organic carbon (TOC) content of sediment is defined as the relative dry weight percentage of organic carbon in its rock or sediment sample (Alaug et al., 2013; Batten, 1996; Durand et al., 1972; Eren and Karakilçik, 2013; Gehman, 1962; M. Hunt, 1979; Jonathan et al., 1976; Sarı, 1994; Sarı and Bozkurt, 2012; Wang et al., 2014). Commonly, it is been agreed that for a rock to be a source of hydrocarbons, it must contain appropriate organic matter to significant generation and expulsion of petroleum or gas. For many years this has been taken as 0.5 wt % TOC for shales and a little less 0.3 wt % TOC for carbonates (Ala et al., 1980; Alizadeh et al., 2012; Basu et al., 1980; Batten, 1996; Dow, 1978; Eren and Karakilçik, 2013; Gehman, 1962; S. Korkmaz and Gedik, 1990; Lafargue et al., 1998; Momper, 1978; K. E. Peters and Cassa, 1994; K. E. Peters and Moldowan, 1993; Sari and Aliyev, 2006; Sarı and Bozkurt, 2012; B. P. Tissot and Welte, 1984). The parameters measured included TOC, S1, S2, S3 and temperature of maximum pyrolysis yield (Tmax). Hydrogen Index (HI) and Oxygen Index (OI) and Production Index (PI) were calculated as described by Espitalié et al. (1977) and K. E. Peters and Cassa (1994) as shown in Table.1.The first peak S1 indicate to the hydrocarbons that can be thermally distilled from a rock and measures the amount of free hydrocarbons that can be yield volatile from the rock without cracking the kerogen (Alaug et al., 2013; LePain et al., 2003; Makky et al., 2014; M. Filho et al., 2012; Nordeng, 2012; K. E. Peters and Cassa, 1994; Sarı et al., 2015). The second peak S2 symbolize the hydrocarbons produced during the Pyrolysis degradation of the kerogen in the rock and calibrate the hydrocarbon yield from cracking the kerogen (mg HC/g rock) and are an important measurement of the generative potential of source rocks (Aliyev et al, 2009; Bordenave, 1993; K. Peters, 1986; K. E. Peters and Cassa, 1994; Sarı et al., 2015; Shalaby et al., 2011). The third peak S3 detects carbon dioxide produced during temperature programming up to 390 °C, and it is resolved using a thermal conductivity detector (TCD) (LePain et al., 2003; Makky et al., 2014; Nordeng, 2012; Sarı and Bozkurt, 2012; Sarı et al., 2015; Sarı and Yarıcı, 2012). The hydrogen index HI represents the quantity of pyrolyzed organic matter from S2 relative to the TOC in the samples (mg HC/g TOC) and it can be used to define the oil generation potential of the rock and the type of the organic matter (Kleinberg and Vinegar, 1996; Sarı et al., 2015). The oxygen index (OI) represents the amount of oxygen relative to the amount of organic carbon present in a sample (Law, 1999). Tmax is the temperature at which the maximum rate of hydrocarbon generation happen in a kerogen sample during pyrolysis analysis (B. P. Tissot et al., 1987). In order to determine the relevance between the elements and organic material, 28 bituminous shale and carbonate rock samples were selected from 54 samples from both Kuşakdağı and Gökçepınar Formations, 22 from the carbonate limestone and 6 from the bituminous shale. Each sample was prepared individually for the geochemical analyses. The analysis involved measuring major, trace and rare earth element abundance as well as determining loss on ignition, TOT/C and TOT/S. About 5g of representative rock sample was broken to pieces with a hardened steel hammer and then packed in a suitable bag and sent to Acme laboratory, Vancouver, Canada, for analysis. Two special measuring device was used for the whole rock geochemical analysis and REE contents of the samples, namely inductively-coupled plasma-emission spectrophotometry (ICP-AES) for major elements and inductively-coupled plasma-mass spectrophotometry (ICP-MS) for trace and rare earth elements. Loss on ignition (LOI) was found by igniting 400 mg of each sample split at 1,000°C and then measuring the weight loss.

IV. Results and discussion

4.1. Rock-Eval pyrolysis, TOC, oil yield and Kerogen types

The organic carbon richness of the source rock sample, as mentioned by the weight percent of TOC content, is useful in the estimation of sediments as a source of petroleum or gas. During the past few years (D. M. Jarvie et al., 2007; Makky et al., 2014; K. Peters, 1986; K. E. Peters and Cassa, 1994; B. P. Tissot and Welte, 1984) introduced a scale for the evaluation of source rocks potentiality, depending on the TOC and Rock Eval pyrolysis data Table. 2. Maturity is the chemical change that occurs in the organic matter composition because of the changes in temperature throughout the burying procedure of sediments that leads to a lot of changes in the organic matter (Douglas and Williams, 1981; Koralay, 2014). Twenty samples from Kuşakdağı were selected for the Rock-Eval pyrolysis analysis to determine the quantity, quality and thermal maturity of the organic matter. The total organic carbon contents of 20 carbonaceous rocks range from 0.13 % to 4.15 % with an average value of 0.698 %. In the pyrolysis analysis, free hydrocarbons (S1), hydrocarbons released from the thermal degradation of kerogen (S2) and the related Tmax values were measured. Various parameters were then calculated using these values Table. 1. Tmax values that been evaluated with pyrolysis analysis are attached to the thermal development of an organic matter (S. Korkmaz et al., 2008; B. Tissot and Espitalie, 1975; B. P. Tissot and Welte, 1984). The HI indicates to the residual generation potential of organic matter and Tmax refers to the temperature at the peak of hydrocarbon generation. Both HI and Tmax from Rock-Eval pyrolysis are useful to characterize the quality and maturity of potential source rocks (Cooles et al., 1986; Espitalié et al.,

1985; D. Jarvie and Tobey, 1999; Katz, 1983; Makky et al., 2014; K. Peters, 1986). Samples with Tmax values below 430°C are described as immature, those with Tmax values between 430–460°C are mature, and those with Tmax values higher than 460°C are over mature source rock (B. P. Tissot and Welte, 1984). Tmax values measured in the Permian units are between 443°C–534°C. These values denote that organic material within the Late Permian samples is the over mature stage. However, Tmax values may change depending on maturity and influence of kerogen (J. Hunt, 1996; Shalaby et al., 2011). According to HI versus TOC diagram represented by Jackson et al. (1985), all the samples have very low HI values suggesting that the organic matter in the studied samples is in gas prone (Fig. 6-a). In the S2-TOC source rock assessment diagram Dembicki Jr (2009), all of the bituminous carbonates samples are of poor source rock potential and rarely of fair and good source rock potential (Fig. 6-b). The type of organic matter has also been determined according to the modified van Krevelen plot of whole rock Hydrogen Index (S2/ TOC × 100) and Oxygen Index (S3/TOC × 100) (Bordenave, 1993; K. Peters, 1986; B. P. Tissot and Welte, 1984) show that most of the Kuşakdağı Formation samples are classified as containing Type III kerogen (Fig.7-a).The kerogen type and maturity of Kuşakdağı Formation samples were also determined using HI versus Tmax diagram (Espitalié et al., 1977; Mukhopadhyay et al., 1995) (Fig. 7-b). Potential yield is the total amount of the free HC and HC generated by the cracking of kerogen in the source rock (Bostick, 1979; Hoş-Çebi and Korkmaz, 2013; Stach, 1982). The PY estimation (S1+S2) have been done in the rock samples to indicate the hydrocarbon generation potential. PY values of the Kuşakdağı Formation were found between 40-520 mgHC/g rock Table. 1. According to B. P. Tissot and Welte (1984), this values refer to a very poor source rock potential. However, the data acquired from the pyrolysis analyses, S1 and S2 values and HI values of the samples are very low. This lead us to conclude that the most amount of the organic matter in these rock samples is composed of residual organic matter. Based on S2/S3 Table. 3 and HI Table. 4 K. E. Peters and Cassa (1994), HI-Tmax (Fig. 7-a), HI-OI (Fig. 7-b) parameters and organic petrographic analysis, the kerogen types of bituminous rocks of Kuşakdağı Formation are Type-III and Type-IV species. The results obtained from TOC and pyrolysis data indicates that the bituminous carbonates samples of the Kuşakdağı Formation are of poor source rock potential and rarely of fair or good source rock potential and the organic material within the Permian samples are of Type-III and Type-IV kerogen at the mature-over mature stage of maturation. Comparable results were obtained by S. Korkmaz and Gedik (1990), who investigated the organic matter content, type, and maturity and source rock potential of the Lower Paleozoic sequences exposed on the Taurus Belt.

4.2. Distribution of major elements

The concentrations of major elements in 28 samples from the Kuşakdağı and Gökçepınar Formations that were studied, in comparison to those of average shale composition (ASC) from Clarke (1924), North American Shale Composite (NASC) from Gromet et al. (1984) and PAAS from Taylor and McLennan (1985), are given in Table. 5. According to Bhatia (1983) and Roser and Korsch (1986), the benefit of major element geochemistry of sedimentary rocks is to define tectonic setting based on discrimination diagrams. An initial evaluation of the values in Table. 5 show that LOI and CaO content generally compose more than 95 wt% of the rock composition (except in samples K 3, K 5 and K 11 high SiO_2 values), and this means that the carbonate phases are the predominating phases in the rock. The content of MgO is close to the average Value of ASC, NASC and PAAS; while, Al_2O_3 , SiO_2, Fe_2O_3, Na_2O, TiO_2, MnO, P_2O_5 and K_2O contents are Lower from them. The average contents of CaO are higher than those of ASC, NASC and PAAS for the high proportion of calcite. The insoluble part of the sediments like, SiO_2 (0.71-8.57 wt%, except in sample K3, K5,K6, K11), Al_2O_3 (0.25-2.55 wt%, except in sample K3, K15, K11) and K_2O (0.04-1.37 wt%) Fe_2O_3 (0.16 – 3.53 wt%, except in sample K11), MgO (0.29-0.95 wt% except in sample T1, T3) have considerably low abundance, while TiO_2, MnO, P_2O_5, Cr_2O_3 and Na_2O concentration are negligible Table. 5. Considerably, the poor abundance of Fe, Mn and P in the samples are probably because of the low detrital and organic effects (Tucker, 1983). The total carbon values are generally high (6.89-13.07 wt%, avg. 12.15 wt%) as expected for carbonate-bearing rocks, while the total sulfur concentration is generally below the 0.59 wt% detection limit.

4.2.1. Major element geochemistry

Roser and Korsch (1988) discriminant function analysis has been applied for provenance investigation of the Kuşakdağı and Gökçepınar samples. On this diagram, the analyzed data plot in the Intermediate igneous provenance field (Fig. 8). K_2O/Na_2O ratio ranges between 0.8 and 11.5 Table. 6, which is much larger than that of ASC (0.4) and NASC (0.29). This indicates that Na is probably replaced by K during the later period of diagenesis (Fedo et al., 1995) or migrates in the process of weathering (Tao et al., 2016). Major oxides were normalized using PAAS values (Taylor and McLennan, 1985) and are shown as spider diagram (Fig. 9). As it is expected of carbonate rocks it can be noticed that Cao and LOI have higher values in comparison to PAAS, while other major elements values are lower than of the PAAS values. Al_2O_3/TiO_2 ratios of most clastic rocks are fundamentally used to define the source rock compositions Oni et al. (2014), because the ratio Al_2O_3 / TiO_2

increases from 3 to 8 for mafic igneous rocks, from 8 to 21 for intermediate rocks, and from 15 to 70 for felsic igneous rocks (Hayashi et al., 1997). As shown in Table. 6 all of the samples have an Al_2O_3/TiO_2 ratio above 10 with an average of 19 that suggest the source rock is intermediate igneous rock. In order to have a knowledge about the pre-metamorphic conditions of the parent materials of the carbonate rocks, the values of the samples were plotted on discrimination diagrams. All of the samples were plotted in the sedimentary field on the Na_2O / Al_2O_3 *cf* K_2O/ Al_2O_3 diagram Garrels (1971) (Fig. 10), suggesting that the carbonate rocks are of sedimentary origin. The carbonate rocks of Kuşakdağı and Gökçepınar Formations are characterized by low Na_2O values. According to Davou and Ashano (2009), a low concentration of Na_2O indicates a shallow, near-shore, low energy "clean water" marine environment of deposition. The ratio (Al/Al+Fe+Mn) is an excellent index for clastic addition to metalliferous sediments,because Al originate from debris as these elements have a good stableness in hydrothermal liquids (Rantitsch et al., 2003). All of the samples have Al/Al+Fe+Mn) > 0.2 Table. 6, suggesting the majority of a pelagic terrigenous constituent characterized by a geochemical composition similar to the average continental crust (Boström, 1973).

4.3. Distribution of trace elements

The trace elements geochemical data of the carbonate rocks in comparison to the PAAS values of Taylor and McLennan (1985) and the NASC values are shown in Table. 7. The average values of Sc, Cu, Pb, Ni, Ba, Co, Cs, Ga, Hf, Nb, Rb, Ta, Th, V, Zr is low in comparison to PAAS and NASC values, whereas Sr average values is higher than both of them. Zn shows higher average values than NASC but lower than PAAS, whereas U is more or less equal to PAAS and NASC values. .

4.3.1. Trace elements geochemistry

Trace elements were normalized using PAAS values Taylor and McLennan (1985) and are shown as spider diagram (Fig. 11). The PAAS normalized patterns of the samples show a moderate to low depletion in Sc, Cu, Pb, Ni, Ba, Co, Cs, Ga, Hf, Nb, Rb, Ta, Th, V, Zr and Zn (except sample T2 which has a higher Pb value than PAAS) , whereas Sr contents are higher than PAAS values. During the last few years, Sr/Cu ratio is widely used to indicate the paleoclimate conditions. Generally, a warm-humid climate is noticed as Sr/Cu ratios ranges between 1.3 and 5.0, whereas Sr/Cu > 5.0 ratios suggest a dry hot climate (Lerman, 1978). The ratios are in the range of 23,22– 1025,58, indicating a very dry hot climate. Also, because of the high Sr/Cu ratios, all of the samples have a high Sr/Ba ratios, Sr/Ba ratios, suggesting a saline water environment (Tao et al., 2016) Table. 6. The high ratios of V/V+Ni (2.1 – 36.7; Table. 6) indicate the presence of H2S in a strongly stratified water column (Hatch and Leventhal, 1992). The abundances of elements such as Sc in sedimentary rocks could appear because of the abundances in the upper continental crust (Götze, 1998). Immobile trace elements in detrital sediments have also been used successfully in discrimination diagrams of paleo-tectonic settings. The discriminate diagram of Th-Sc-Zr/10 and Th-Co-Zr/10 ternary diagrams Bhatia and Crook (1986) used indiscriminately the samples of Kuşakdağı and Gökçepınar Formations to recognize if they are derived from oceanic island arcs, continental island arcs and active or passive continental margins. These criteria must be used with caution as some sediments are transported from their tectonic setting of origin into a sedimentary basin in a different tectonic environment (Bauluz et al., 2000).Using this diagram (Fig. 12), it was concluded that most of the samples were deposited in the continental island arcs field. The differentiation diagram of Th/Sc-Z/Sc after S. McLennan et al. (1993) is widely used to indicate the composition of the source rock. This diagram provides information about the degree of fractionation of the source rocks. The plot of Th/Sc versus Zr/Sc diagram as shown in (Fig. 13), indicates most of the sediments found in the zone of lower continental crust.

4.4. Distribution of REE

The data on REEs concentrations in comparison to the PAAS values of Taylor and McLennan (1985) and the NASC values are presented in Table. 8. The average ΣREE concentrations of the samples is 52.65 ppm. The variety in the amount of terrigenous sediment enrichment in these samples, cause to differences in ΣREE content between the carbonate rock samples. The content of almost all of the REE is lower than that of NASC and PAAS values. The content of the total rare earth elements (ΣREE) shows a high variation, ranging from 7.31 to 258.3 PPM Table. 8. The average value is 52.6 ppm, which is higher than that of NASC and PAAS average values. A cursory appraisal of the PAAS and NASC normalized rare earth element plots indicates that all the samples have similar REE patterns, with moderate to strong fractionation of light rare earth elements over heavy rare earth elements, that is incompartible with the common distribution of REEs in carbonate rocks (Gromet et al., 1984; Taylor and McLennan, 1985). The LREE/HREE ratios range from 1.82 to 8.70 with an average value of 4.09 Table. 6, which is higher than the average value of NASC (3.77 PPM) and lower than the average value of PAAS (4.3 PPM).

4.4.1. REE geochemistry

REE concentrations are normalized to PAAS values Taylor and McLennan (1985) in (Fig. 14) and NASC values in (Fig. 15). The abundance and decreasing of REE content in carbonate rocks can be effected by different factors, 1) contribution of terrigenous grains from the continent (S. M. McLennan, 1989; Nagarajan et al., 2011; Piper, 1974), 2) authigenic depletion of REE from the water column and early diagenesis (J. Madhavaraju and Ramasamy, 1999; Sholkovitz, 1988), 3) scavenging process relative to depth, salinity and oxygen levels (Bertram and Elderfield, 1993; H. Elderfield et al., 1988; Greaves et al., 1999; Piepgras and Jacobsen, 1992) and 4) biogenic sedimentation from the overlying seawater (Murphy and Dymond, 1984; Murray et al., 1991). During the last few years, Yttrium was put between Ho and Dy in the REE pattern according to its identical charge and similar radius (Bau, 1996). The carbonate rocks of the Kuşakdağı and Gökçepınar Formations show large variations in Y/Ho ratios (22.6 - 63.3) Table. 6. The noticed differences in the Y/Ho ratios suggest that the samples were polluted by the effect of terrigenous materials (Nagarajan et al., 2011). Europium anomaly, generally expressed by [Eu/Eu∗], and can be estimated by comparison of normalized Eu concentration with an expected concentration (Eu∗). in this study the europium anomaly is given by (Taylor and McLennan, 1985);

Eu/Eu* = EuN / [(SmN × GdN)]1/2,

Where N stands for the normalization of REEs to PAAS.

The REE patterns of the samples correlative to PAAS are shown in (Fig. 14) and to NASC in (Fig. 15). All of the samples (except K11) shows a slight positive Eu anomaly, suggesting a moderate depositional environment (Berger et al., 2014). The Eu anomalies are useful to grasp the physical and chemical circumstance of different geological systems (Derry and Jacobsen, 1990; Dymek and Klein, 1988; Walker et al., 1983). Values higher than 0.85 indicate positive Eu anomaly, values lower than 0.85 indicate a negative Eu anomaly, and a value of exactly 0.85 indicates no anomaly (Oni et al., 2014). In this study as shown in Table. 6, the samples show a positive Eu anomaly (Eu/Eu*), which range from (0.81 to 1.41 normalized by PAAS values with an average of 1.01, and from 0.72 to 1.28 by NASC values with an average of 0.90). According to (C. German et al., 1993; Kurian et al., 2008; MacRae et al., 1992; J. Madhavaraju and Lee, 2009; Michard et al., 1983; Murray et al., 1991; Nath et al., 1992), the positive Eu anomalies are mainly generated in sediments affected by hydrothermal processes, intense diagenesis or variations in plagioclase content. The use of cerium anomaly was first proposed by H. Elderfield and Greaves (1982) as a result of the change in the ionic state of Ce as a function of oxidation state and is defined in several ways (Sholkovitz, 1988; Wright et al., 1987). The Ce anomaly specifies the relative attitude of Ce according to the neighboring LREEs and are used to demonstrate geochemistry settings in distinct aspects. For calculation of Ce anomalies, the corresponding values were normalized to post-Archean Australian shale (PAAS) by using the following formula (Taylor and McLennan, 1985):

$Ce/Ce^* = 2Ce_N / (La_N + Pr_N)$, where N stands for the normalization of REEs to PAAS.

The samples show positive Ce/Ce* anomaly with a range of (0.57 – 1.12 with an average of 0.9 normalized by PAAS values, and 0.58 – 1.14 with an average of 0.91 normalized by NASC values; Table. 6). In general, the positive anomaly of Ce can be generated due to factors like, lithology and diagenesis, paleoredox conditions, Fe-organic REE rich colloids from the fluvial input and can occur as a result of terrigenous influence to the sediment (Armstrong-Altrin et al., 2003; C. R. German and Elderfield, 1990; J. Madhavaraju and Ramasamy, 1999; Nath et al., 1992; Sholkovitz, 1992).

Wright et al. (1987) suggested the following formula for calculating the Ce anomaly:

$Ce_{anom} = Log\ (3Ce_n/(2La_n+Nd_n))$, Where Ce_n, La_n, and Nd_n are obtained by chondrite-normalized value.

Ce anomaly with negative or positive signature is present, with the values ranging from -2.9 to 0.08 as seen in Table. 6. These values are plotted on the Ce anomaly vs. Nd concentration diagram and it shows that most of the samples are found in the anoxic conditions with a moderate sedimentation speed (Fig. 16). In this study, the Hf-La/Th discrimination diagram that suggested by Floyd and Leveridge (1987), is applied for the differentiation of the provenance of the samples (Fig. 17). The samples are plotted in a different field of andesitic provenance, and that advocates the intermediate igneous provenance of the samples. The normalization of REE to NASC (Fig. 15), shows that all of the samples have similar patterns that do not vary essentially in either sample. All of the samples show a flat trend without apparent anomaly, suggesting that these samples were deposited in an identical sedimentary environment with similar epigenetic evolution and the REE fractionation was not effected by diagenesis (Li et al., 2008).

V. Geochemical interrelationships

The Geochemical interrelationships of the major element oxides and trace elements of the Kuşakdağı and Gökçepınar carbonate rock samples have been studied and the results given as correlation coefficients Table. 9 and covariation plots (Fig. 18). As shown in Table. 9, and (Fig. 18) the concentration of SiO_2 and Al_2O_3

are decreased with increasing CaO content in the rock and shows a strong negative correlation between them (r = - 0.986, r = - 0.977 respectively). However, the CaO composition shows a negative correlation with Fe_2O_3, TiO_2, K_2O, Cr_2O_3, Na_2O and P_2O_5, (r = - 0.952, r = - 0.986, r = - 0.965, r = - 0.967, r = - 0.823, r = - 0.947 respectively) (Fig. 18) on the other hand SiO_2 display a positive correlation with Al_2O_3, Fe_2O_3 and K_2O (r = 0.985, r = 0.912, r = 0.973 respectively). Also TiO_2 shows a positive correlation with SiO_2, Al_2O_3 and Fe_2O_3 (r = 0.982, r = 0.994, r = 0.866 respectively) (Fig. 19). In addition, there is a very weak positive correlation between CaO with MgO and MnO compositions (r = 0.27, r = 0.6 respectively) (Fig. 19). The decreasing in SiO_2 content with increasing of CaO concentration of the rock samples (Fig. 18) suggesting that the rock contains different silicate and carbonate components (Ephraim, 2012). The indicated positive relationship between SiO_2 and Al_2O_3, and the negative correlation display between CaO and the different insoluble residues (Fig. 18) suggest that the non-carbonate portion of the rock samples are largely aluminosilicates and that CaO in contrast with the other oxides of the carbonate rocks, exhibit different modes of origin (Abedini and Calagari, 2015). In order to estimate the origin of the carbonate rock samples, the bivariate plots of the major oxides and the percentage of clastic materials existent in the carbonate rocks have been used (Cullers, 2002; Parekh et al., 1977). The excellent linear correlation display between $\sum(SiO_2+Al_2O_3+ Fe_2O_3+ Na_2O+K_2O+ TiO_2)$ and the percentage of clastic materials and the negative correlation between CaO and LOI with the percentage of clastic materials (Fig. 20 a, b and c) (r = 1, r = - 0.989, r = - 0.982 respectively), indicate that these oxides are mainly incorporated into the clastic materials rather than the calcite, and the carbonate materials are incorporated into the carbonate phase. The terrigenous source for REEs in carbonate rocks can be indicated by the correlation coefficients between REEs and certain major and trace elements (Abedini and Calagari, 2015). Positive correlation of ΣREE with Al_2O_3 and the negative correlation of ΣREE with CaO (Fig. 19 d and e) (r = 0.964, r = - 0.914 respectively), indicate to the appearance of the terrigenous component, that could be the origin of REE in these carbonate rocks. The Ce/Ce* values show a weak positive or negative correlation with U and CaO (Fig. 20 a, b) (r = 0.25, r = - 0,3 respectively), suggesting that the changes in Ce anomalies are not affected by the paleoredox climate of the depositional environment. The Ce/Ce* values also have a linear or a very weak positive correlations with Mn, Fe and Pb (Fig. 20 f, g, h) (r = 0.153, r = 0.117, r = 0.318 respectively). Suggesting that this carbonate rock samples were precipitated in a mid to shallow marine environment. The Ce/Ce* values have a linear or a very weak positive correlations with Si and Zr (Fig. 21 c, d) (r = 0.366, r = 0.253 respectively), Suggesting that the Ce enrichment and Ce anomaly of this carbonate rocks are not affected so much by the material entrance to the basin. The positive correlation between Eu and Al_2O_3 (Fig. 22 a) (r = 0.828), content suggest the detrital origin of this element. The Eu/Eu* values display a very weak negative correlations with Zr, Y, Th, Hf (Fig. 22 b, c, d, e) (r = - 0.338, r = - 0.29, r = - 0.267, r = - 0.327 respectively), suggesting that the occurrence of Eu anomalies in the samples studied is not effected by the diagenesis processes (J. Madhavaraju and Lee, 2009). Recently, trace elements such as Th and Sc used as indicators of carbonate rocks contamination (Webb and Kamber, 2000). The Th and Sc shows a very strong positive correlation with Al_2O_3 contents (Fig. 23 a, b) (r = 0,988), which advocate the presence of shale contamination in the carbonate rock samples of Kuşakdağı and Gokçepınar Formations.

VI. Conclusions

In order to get a better knowledge of the oil generation characteristics of Kuşakdağı samples, a combined investigation of organic geochemistry and organic petrology had been applied. For this reason, Rock-Eval pyrolysis data is used to determine the organic matter content, types of organic matter, thermal maturation level and the source rock potential of the Late Permian Kuşakdağı Formation. In addition, the geochemistry of the Late Permian Kuşakdağı and Lower Triassic Gökçepınar Formations were also studied. The results obtained from Rock-Eval pyrolysis analysis indicates that the organic matter of the Late Permian Kuşakdağı Formation contains Type III kerogen (Vitrinite) and Type IV kerogen (Inertinite). The Corg amounts of the source rock terrigenous material in the Kuşakdağı Formation carbonate rocks range from 0.13 % to 4.15 % with an average value of 0.698 %, consistent with having poor source rock potential and that advocated by the low S1, S2 and HI values. According to the data obtained from HI-Tmax and S2-TOC diagrams, the Kuşakdağı carbonate rocks are plotted within the fields characteristic for Type III and Type IV kerogen field with a poor source rock potential. The maturity of the Kuşakdağı samples was estimated by the Tmax values. According to Tmax and PI values, the samples are generally of over mature stage. Potential yield (PY) values of the Kuşakdağı Formation were found between 40-520 mgHC/g, indicating that the samples are having a very low hydrocarbon generation potential. Positive correlation of ΣREE with Al_2O_3 and negative correlation of ΣREE with CaO indicate to the existence of terrigenous fractions, that is may be the source for REE in these carbonate rocks. The high CaO content in these samples refer to the high proportion of calcite in these carbonate rocks. The observed high K_2O/ Na_2O ratios are because of the K-metasomatism. All of the samples have an Al_2O_3 / TiO_2 ratio above 10 with an average of 19 which is an indication that the source rock is felsic or intermediate igneous rock. The REE contents in the carbonate rocks of Kuşakdağı and Gökçepınar Formations are very low compared to the PAAS

and the NASC values. The strong positive correlation of REEs with elements such as Si, Al, Ti, V, Co, Ni, Rb, Cu, and Nb, and the negative correlation between REEs and CaO, suggest that the distribution of REEs in the studied carbonate rocks are controlled by the terrigenous materials. Trace element ratios of the immobile elements such as Th, Zr, Co and Sc can be used to indicate the provenance signature. Using the discrimination plots Th-Co-Zr/10, Th-Sc-Zr/10 according to Bhatia and Crook (1986), the analyzed samples are typical of the continental island arcs and partially of the oceanic island arcs tectonic settings. The results suggest that the samples of Kuşakdağı and Gökçepınar Formations were derived from intermediate igneous provenance and they are deposited in a mid to shallow saline water environment with hot-dry climates and anoxic conditions.

Acknowledgments

We would like to thank anonymous reviewer for the detailed comments and discussions that helped to improve the manuscript. We would also like to thank Dr. Ahmet Turan for his time and help in the geological work of the study area. We would also like to thank our families for their continuous support.

References

[1]. Abedini, A., and Calagari, A., 2015. Rare earth element geochemistry of the Upper Permian limestone: the Kanigorgeh mining district, NW Iran. Turkish Journal of Earth Sciences, 24 (4), 365-382.
[2]. Ala, M., Kinghorn, R., and Rahman, M., 1980. Organic geochemistry and source rock characteristics of the Zagros petroleum province, southwest Iran. Journal of Petroleum Geology, 3 (1), 61-89.
[3]. Alaug, A., Batten, D., and Ahmed, A., 2013. Organic geochemistry, palynofacies and petroleum potential of the Mukalla Formation (late Cretaceous), Block 16, eastern Yemen. Marine and Petroleum Geology, 46, 67-91.
[4]. Aliyev, S., Sarı, A., Koralay, D., and Koç, Ş., 2009. Investigation of organic carbon and trace metal enrichments of rocks at the Paleocene-Eocene boundary, NW Turkey. Petroleum Science and Technology, 27 (1), 56-71.
[5]. Alizadeh, B., Sarafdokht, H., Rajabi, M., Opera, A., and Janbaz, M., 2012. Organic geochemistry and petrography of Kazhdumi (Albian–Cenomanian) and Pabdeh (Paleogene) potential source rocks in southern part of the Dezful Embayment, Iran. Organic geochemistry, 49, 36-46.
[6]. Armstrong-Altrin, J., Verma, S., Madhavaraju, J., Lee, Y., and Ramasamy, S., 2003. Geochemistry of upper Miocene Kudankulam limestones, southern India. International Geology Review, 45 (1), 16-26.
[7]. Banner, J., Hanson, G., and Meyers, W., 1988. Water-rock interaction history of regionally extensive dolomites of the Burlington-Keokuk Formation (Mississippian): isotopic evidence. 43, 97-113.
[8]. Basu, D., Banerjee, A., and Tamhane, D., 1980. Source areas and migration trends of oil and gas in Bombay offshore basin, India. AAPG Bulletin, 64 (2), 209-220.
[9]. Batten, D., 1996. Palynofacies. Palynology: principles and applications, 3, 1011-1084.
[10]. Bau, M., 1996. Controls on the fractionation of isovalent trace elements in magmatic and aqueous systems: evidence from Y/Ho, Zr/Hf, and lanthanide tetrad effect. Contributions to Mineralogy and Petrology, 123 (3), 323-333.
[11]. Bauluz, B., Mayayo, M., Fernandez-Nieto, C., and Lopez, J., 2000. Geochemistry of Precambrian and Paleozoic siliciclastic rocks from the Iberian Range (NE Spain): implications for source-area weathering, sorting, provenance, and tectonic setting. Chemical Geology, 168 (1), 135-150.
[12]. Berger, A., Janots, E., Gnos, E., Frei, R., and Bernier, F., 2014. Rare earth element mineralogy and geochemistry in a laterite profile from Madagascar. Applied geochemistry, 41, 218-228.
[13]. Bertram, C., and Elderfield, H., 1993. The geochemical balance of the rare earth elements and neodymium isotopes in the oceans. Geochimica et Cosmochimica Acta, 57 (9), 1957-1986.
[14]. Bhatia, M. R., 1983. Plate tectonics and geochemical composition of sandstones. The Journal of Geology, 91 (6), 611-627.
[15]. Bhatia, M., and Crook, K., 1986. Trace element characteristics of graywackes and tectonic setting discrimination of sedimentary basins. Contributions to Mineralogy and Petrology, 92 (2), 181-193.
[16]. Blumenthal, M., 1944. Bozkır güneyinde Toros sıradağlarının serisi ve yapısı. İÜ FF Mec., seri: B, 9, 95-125.
[17]. Blumenthal, M., 1951. Batı Toroslar'da Alanya ard ülkesinde jeolojik araştırmalar. MTA derg., seri: D, 5, 194.
[18]. Blumenthal, M., and Göksu, E., 1949. Batı Torosların ört lamboları. Türkiye Jeol. Kur. Bült, 2 (1), 30-40.
[19]. Bordenave, M., 1993. Applied petroleum geochemistry: Technip Paris.
[20]. Bostick, N., 1979. Microscopic measurement of the level of catagenesis of solid organic matter in sedimentary rocks to aid exploration for petroleum and to determine former burial temperatures. SEMP, sp. Publ.,, 26,, 17-43.
[21]. Boström, K., 1973. The origin and fate of ferromanganoan active ridge sediments: Stockholm Contributions to Geology, v. 27.
[22]. Chen, S., Gui, H., and Sun, L., 2014. Geochemical characteristics of REE in the Late Neo-proterozoic limestone from northern Anhui Province, China. Chinese Journal of Geochemistry, 33 (2), 187-193.
[23]. Clarke, F., 1924. The data of geochemistry. US Geol. Surv., Bull., 770.
[24]. Condie, K., 1993. Chemical composition and evolution of the upper continental crust: contrasting results from surface samples and shales. Chemical Geology, 104 (1-4), 1-37.
[25]. Cooles, G., Mackenzie, A., and Quigley, T., 1986. Calculation of petroleum masses generated and expelled from source rocks. Organic geochemistry, 10 (1-3), 235-245.
[26]. Cullers, R. L., 2002. Implications of elemental concentrations for provenance, redox conditions, and metamorphic studies of shales and limestones near Pueblo, CO, USA. Chemical Geology, 191 (4), 305-327.
[27]. Davou, D., and Ashano, E., 2009. The geochemical chararateristics of the marble deposits east of Federal Capital Territory (FCT), Nigeria. Global Journal of Geological Sciences, 7 (2), 189-198.
[28]. Dembicki Jr, H., 2009. Three common source rock evaluation errors made by geologists during prospect or play appraisals. AAPG Bulletin, 93 (3), 341-356.
[29]. Derry, L., and Jacobsen, S., 1990. The chemical evolution of Precambrian seawater: evidence from REEs in banded iron formations. Geochimica et Cosmochimica Acta, 54 (11), 2965-2977.
[30]. Douglas, A., and Williams, P., 1981. Kimmeridge oil shale, a study of organic maturation. Organic maturation studies and fossil fuel exploration. Academic, London, 255-269.
[31]. Dow, W., 1978. Petroleum source beds on continental slopes and rises. AAPG Bulletin, 62 (9), 1584-1606.

[32]. Durand, B., Espitalié, J., Nicaise, G., and Combaz, A., 1972. Etude de la matière organique insoluble (kérogène) des argiles du Toarcien du Bassin de Paris. Premiere partie-Etude par les procédés optiques. Analyse élémentaire. Etude en microscopie et diffraction électroniques: Rev. Inst. Franc. Pétrole, 27, 865-884.
[33]. Dymek, R., and Klein, C., 1988. Chemistry, petrology and origin of banded iron-formation lithologies from the 3800 Ma Isua supracrustal belt, West Greenland. Precambrian Research, 39 (4), 247-302.
[34]. Elderfield, H., and Greaves, M. J., 1982. The rare earth elements in seawater. Nature, 296, 214-219.
[35]. Elderfield, H., Upstill-Goddard, R., and Sholkovitz, E., 1990. The rare earth elements in rivers, estuaries, and coastal seas and their significance to the composition of ocean waters. Geochimica et Cosmochimica Acta, 54 (4), 971-991.
[36]. Elderfield, H., Whitfield, M., Burton, J., Bacon, M., and Liss, P., 1988. The oceanic chemistry of the rare-earth elements [and discussion]. Philosophical Transactions of the Royal Society of London A: Mathematical, Physical and Engineering Sciences, 325 (1583), 105-126.
[37]. Ephraim, B., 2012. Investigation of the geochemical signatures and conditions of formation of metacarbonate rocks occurring within the Mamfe embayment of south-eastern Nigeria. Earth Sciences Research Journal, 16 (2), 121-138.
[38]. Eren, V., and Karakilçik, H., 2013. Investigation of Oil Resource Potentıal of the South East of the Diyarbakır Provıence‘s Bismil District with Geological and Geophysical Methods. Ç.Ü Fen ve Mühendislik Bilimleri Dergisi, Cilt:29-3, 98-106.
[39]. Espitalié, J., Deroo, G., and Marquis, F., 1985. La pyrolyse Rock-Eval et ses applications. Deuxième partie. Revue de l'Institut français du Pétrole, 40 (6), 755-784.
[40]. Espitalié, J., Laporte, J., Madec, M., Marquis, F., Leplat, P., Paulet, J., and Boutefeu, A. 1977. Méthode rapide de caractérisation des roches mètres, de leur potentiel pétrolier et de leur degré d'évolution. Revue de l'Institut français du Pétrole, 32 (1), 23-42.
[41]. Fedo, C., Nesbitt, W., and Young, G., 1995. Unraveling the effects of potassium metasomatism in sedimentary rocks and paleosols, with implications for paleoweathering conditions and provenance. Geology, 23 (10), 921-924.
[42]. Floyd, P., and Leveridge, B., 1987. Tectonic environment of the Devonian Gramscatho basin, south Cornwall: framework mode and geochemical evidence from turbiditic sandstones. Journal of the Geological Society, 144 (4), 531-542.
[43]. Frimmel, H., 2009. Trace element distribution in Neoproterozoic carbonates as palaeoenvironmental indicator. Chemical Geology, 258 (3), 338-353.
[44]. Fu, X., Wang, J., Zeng, Y., Tan, F., and He, J., 2011. Geochemistry and origin of rare earth elements (REEs) in the Shengli River oil shale, northern Tibet, China. Chemie der Erde-Geochemistry, 71 (1), 21-30.
[45]. Garrels A., and Mackenzie, F., 1971, Evolution of sedimentary rocks: Norton and Company, Inc., New York, NY.
[46]. Gehman, H., 1962. Organic matter in limestones. Geochimica et Cosmochimica Acta, 26 (8), 885-897.
[47]. German, C., Higgs, N., Thomson, J., Mills, R., Elderfield, H., Blusztajn, J., and Bacon, M., 1993. A geochemical study of metalliferous sediment from the TAG Hydrothermal Mound, 26° 08′ N, Mid-Atlantic Ridge. Journal of Geophysical Research: Solid Earth, 98 (B6), 9683-9692.
[48]. German, C., and Elderfield, H., 1990. Application of the Ce anomaly as a paleoredox indicator: the ground rules. Paleoceanography, 5 (5), 823-833.
[49]. Goldberg D., Koide, M., Schmitt, R., and Smith, R., 1963. Rare-Earth distributions in the marine environment. Journal of Geophysical Research, 68 (14), 4209-4217.
[50]. Göktepe, G., and Güvenç, T., 1997. Hadim napı Üst Permiyen stratigrafisi ve paleontolojisi; ÇÜ ′de Jeoloji Mühendisliği Eğitiminin 20. Yılı Simp., bildiri özleri, 213-214.
[51]. Götze, J., 1998. Geochemistry and provenance of the Altendorf feldspathic sandstone in the Middle Bunter of the Thuringian basin (Germany). Chemical Geology, 150 (1), 43-61.
[52]. Greaves, M., Elderfield, H., and Sholkovitz, E., 1999. Aeolian sources of rare earth elements to the Western Pacific Ocean. Marine Chemistry, 68 (1), 31-38.
[53]. Gromet, L., Haskin, L., Korotev, R., and Dymek, R., 1984. The “North American shale composite”: its compilation, major and trace element characteristics. Geochimica et Cosmochimica Acta, 48 (12), 2469-2482.
[54]. Haskin, L., Haskin, M., Frey, F., and Wildeman, T., 1968. Relative and absolute terrestrial abundances of the rare earths. Origin and Distribution of the Elements, 1, 889-911.
[55]. Haskin, M., and Haskin, L., 1966. Rare earths in European shales: a redetermination. Science, 154 (3748), 507-509.
[56]. Hatch, J., and Leventhal, J., 1992. Relationship between inferred redox potential of the depositional environment and geochemistry of the Upper Pennsylvanian (Missourian) Stark Shale Member of the Dennis Limestone, Wabaunsee County, Kansas, USA. Chemical Geology, 99 (1-3), 65-82.
[57]. Hayashi, K., Fujisawa, H., Holland, H., and Ohmoto, H., 1997. Geochemistry of 1.9 Ga sedimentary rocks from northeastern Labrador, Canada. Geochimica et Cosmochimica Acta, 61 (19), 4115-4137.
[58]. Hoş-Çebi, F., and Korkmaz, S., 2013. Organic geochemistry and depositional environments of Eocene coals in northern Anatolia, Turkey. Fuel, 113, 481-496.
[59]. Hua, G., Yuansheng, D., Lian, Z., Jianghai, Y., Hu, H., Min, L., and Yuan, W., 2013. Trace and rare earth elemental geochemistry of carbonate succession in the Middle Gaoyuzhuang Formation, Pingquan Section: implications for Early Mesoproterozoic ocean redox conditions. Journal of Palaeogeography, 2 (2), 209-221.
[60]. Hunt, J., 1996. Petroleum geology and geochemistry: New York, Freeman and Company.
[61]. Hunt, M., 1979. Petroleum geochemistry and geology: WH Freeman and company.
[62]. Jackson, K., Hawkins, P., and Bennett, A., 1985. Regional facies and geochemical evaluation of southern Denison Trough. Australian Petroleum Exploration Association Journal, 20, 143-158.
[63]. Jarrar, G., Amireh, B., and Zachmann, D., 2000. The major, trace and rare earth element geochemistry of glauconites from the early Cretaceous Kurnub Group of Jordan. Geochemical Journal, 34 (3), 207-222.
[64]. Jarvie, D., and Tobey, M., 1999. TOC, Rock-Eval and SR Analyzer Interpretive Guidelines Application Note 99-4: Humble Instruments and Services, Inc. Geochemical services Division Texas.
[65]. Jarvie, D., Hill, R., Ruble, T., and Pollastro, R., 2007. Unconventional shale-gas systems: The Mississippian Barnett Shale of north-central Texas as one model for thermogenic shale-gas assessment. AAPG Bulletin, 91(4), 475-499.
[66]. Jonathan, D., Le Tran, K., Oudin, S., and Van der Weide, B., 1976. Les methodesd’physica-chimique de la matire organique. Bull. Centre Rech. Pau. SNPA, 10 (1),, 39-109.
[67]. Katz, B., 1983. Limitations of ‘Rock-Eval’pyrolysis for typing organic matter. Organic geochemistry, 4 (3-4), 195-199.
[68]. Kleinberg, R., and Vinegar, H., 1996. NMR properties of reservoir fluids. The Log Analyst, 37 (06), 20-32.
[69]. Koralay, D., 2014. Organic geochemical and isotopic (C and N) characterization of carbonaceous rocks of the Denizli Area, Western Turkey. Journal of Petroleum Science and Engineering, 116, 90-102.

[70]. Korkmaz, S., and Gedik, A., 1990. Mut-Ermenek-Silifke (Konya-Mersin) havzasında ana kaya fasiyesi ve petrol oluşumunun organik jeokimyasal yöntemlerle incelenmesi. Geological Bulletin of Turkey, 33, 29-38.
[71]. Korkmaz, S., Gülbay, R., and Demirel, İ., 2008. Source Rock Characteristics, Organic Maturity, and Hydrocarbon Potential of the Lower Paleozoic Sequences in the Taurus Belt of Turkey. Petroleum Science and Technology, 26 (16), 1869-1886.
[72]. Kurian, S., Nath, B., Ramaswamy, V., Naman, D., Rao, T., Raju, K., and Chen, C., 2008. Possible detrital, diagenetic and hydrothermal sources for Holocene sediments of the Andaman backarc basin. Marine Geology, 247 (3), 178-193.
[73]. Kuşcu, M., Özsoy, R., Özçelik, O., and Altunsoy, M., 2016. Trace and Rare Earth Element Geochemistry of Black Shales in Triassic Kasimlar Formation, Anamas-Akseki Platform, Western Taurids, Turkey. Paper presented at the IOP Conference Series: Earth and Environmental Science.
[74]. Kuşçu, M., 1983. Göktepe (Ermenek) yöresinin jeolojisi ve Pb-Zn yatakları; SÜ Müh. Mim. Fak. doktora tezi (unpublished), 181.
[75]. Lafargue, E., Marquis, F., and Pillot, D., 1998. Rock-Eval 6 applications in hydrocarbon exploration, production, and soil contamination studies. Revue de l'Institut français du Pétrole, 53 (4), 421-437.
[76]. Law, C., 1999. Treatise of Petroleum Geology/Handbook of Petroleum Geology: Exploring for Oil and Gas Traps. Chapter 6: Evaluating Source Rocks.
[77]. LePain, D., Blodgett, R., and Clough, J., 2003. Sedimentology and hydrocarbon source rock potential of Miocene-Oligocene strata, McGrath Quadrangle: An outcrop analog for the Holitna basin: Division of Geological & Geophysical Surveys.
[78]. Lerman, A., 1978. Lakes: Chemistry, geology, physics. . Springer-Verlag, New York,, 237-289.
[79]. Li, D., Tang, Y., Deng, T., Chen, K., and Liu, D., 2008. Geochemistry of rare earth elements in coal a case study from Chongqing, southwestern China. Energy Exploration & Exploitation, 26 (6), 355-362.
[80]. Liu, Y., Miah, M., and Schmitt, R., 1988. Cerium: a chemical tracer for paleo-oceanic redox conditions. Geochimica et Cosmochimica Acta, 52 (6), 1361-1371.
[81]. MacRae, N., Nesbitt, H., and Kronberg, B., 1992. Development of a positive Eu anomaly during diagenesis. Earth and Planetary Science Letters, 109 (3-4), 585-591.
[82]. Madhavaraju, J., González-León, C., Lee, Y., Armstrong-Altrin, J., and Reyes-Campero, L., 2010. Geochemistry of the mural formation (Aptian-Albian) of the Bisbee group, Northern Sonora, Mexico. Cretaceous Research, 31 (4), 400-414.
[83]. Madhavaraju, J., and Lee, Y. I., 2009. Geochemistry of the Dalmiapuram Formation of the Uttatur Group (Early Cretaceous), Cauvery basin, southeastern India: Implications on provenance and paleo-redox conditions. Revista Mexicana de Ciencias Geológicas, 26 (2), 380-394.
[84]. Madhavaraju, J., and Ramasamy, S., 1999. Rare earth elements in limestones of Kallankurichchi Formation of Ariyalur Group, Tiruchirapalli Cretaceous, Tamil Nadu. Geological Society of India, 54 (3), 291-301.
[85]. Makky, A., El Sayed, M., El-Ata, A., El-Gaied, I., Abdel-Fattah, M., and Abd-Allah, Z., 2014. Source rock evaluation of some upper and lower Cretaceous sequences, West Beni Suef Concession, Western Desert, Egypt. Egyptian Journal of Petroleum, 23 (1), 135-149.
[86]. McLennan, S., Hemming, S., McDaniel, D., and Hanson, G., 1993. Geochemical approaches to sedimentation, provenance, and tectonics. Geological Society of America Special Papers, 284, 21-40.
[87]. McLennan, S., 1989. Rare earth elements in sedimentary rocks; influence of provenance and sedimentary processes. Reviews in Mineralogy and Geochemistry, 21 (1), 169-200.
[88]. Mendonça Filho, J., Menezes, T., de Oliveira Mendonça, J., de Oliveira, A., da Silva, T., Rondon, N., and da Silva, F., 2012. Organic facies: palynofacies and organic geochemistry approaches Geochemistry-Earth's System Processes: InTech.
[89]. Michard, A., Albarede, F., Michard, G., Minster, J., and Charlou, J., 1983. Rare-earth elements and uranium in high-temperature solutions from East Pacific Rise hydrothermal vent field (13 N). Nature, 303 (5920), 795-797.
[90]. Momper, J., 1978. Oil migration limitations suggested by geological and geochemical considerations.
[91]. Morad, S., Al-Aasm, I., Sirat, M., and Sattar, M., 2010. Vein calcite in cretaceous carbonate reservoirs of Abu Dhabi: Record of origin of fluids and diagenetic conditions. Journal of Geochemical Exploration, 106 (1), 156-170.
[92]. Morgan, J., Higuchi, H., Takahashi, H., and Hertogen, J., 1978. A "chondritic" eucrite parent body: Inference from trace elements. Geochimica et Cosmochimica Acta, 42 (1), 27-38.
[93]. Mrkić, S., Stojanović, K., Kostić, A., Nytoft, H., and Šajnović, A., 2011. Organic geochemistry of Miocene source rocks from the Banat depression (SE Pannonian Basin, Serbia). Organic geochemistry, 42 (6), 655-677.
[94]. Mukhopadhyay, P., Wade, J., and Kruge, M., 1995. Organic facies and maturation of Jurassic/Cretaceous rocks, and possible oil-source rock correlation based on pyrolysis of asphaltenes, Scotian Basin, Canada. Organic geochemistry, 22 (1), 85-104.
[95]. Murphy, K., and Dymond, J., 1984. Rare earth element fluxes and geochemical budget in the eastern equatorial Pacific. Nature, 307 (5950), 444-447.
[96]. Murray, R., Brink, M., Brumsack, H., Gerlach, D., and Russ, G., 1991. Rare earth elements in Japan Sea sediments and diagenetic behavior of Ce/Ce∗: Results from ODP Leg 127. Geochimica et Cosmochimica Acta, 55 (9), 2453-2466.
[97]. Murray, R., Ten Brink, M., Gerlach, D., Russ, G., and Jones, D., 1991. Rare earth, major, and trace elements in chert from the Franciscan Complex and Monterey Group, California: Assessing REE sources to fine-grained marine sediments. Geochimica et Cosmochimica Acta, 55 (7), 1875-1895.
[98]. Murray, R., Ten Brink, M., Gerlach, D., Russ, G., and Jones, D., 1992. Interoceanic variation in the rare earth, major, and trace element depositional chemistry of chert: perspectives gained from the DSDP and ODP record. Geochimica et Cosmochimica Acta, 56 (5), 1897-1913.
[99]. Murray, R., Ten Brink, M., Jones, D., Gerlach, D., and Russ, G., 1990. Rare earth elements as indicators of different marine depositional environments in chert and shale. Geology, 18 (3), 268-271.
[100]. Nagarajan, R., Madhavaraju, J., Armstrong-Altrin, J., and Nagendra, R., 2011. Geochemistry of neoproterozoic limestones of the Shahabad formation, Bhima basin, Karnataka, southern India. Geosciences Journal, 15 (1), 9-25.
[101]. Nath, B., Roelandts, I., Sudhakar, M., and Plüger, W., 1992. Rare earth element patterns of the Central Indian Basin sediments related to their lithology. Geophysical Research Letters, 19 (12), 1197-1200.
[102]. Nordeng, S., 2012. Basic geochemical evaluation of unconventional resource plays. Geo News, 39 (1), 14-18.
[103]. Nothdurft, L., Webb, G., and Kamber, B., 2004. Rare earth element geochemistry of Late Devonian reefal carbonates, Canning Basin, Western Australia: confirmation of a seawater REE proxy in ancient limestones. Geochimica et Cosmochimica Acta, 68 (2), 263-283.
[104]. Oni, S., Olatunji, A., and Ehinola, O., 2014. Determination of Provenance and Tectonic Settings of Niger Delta Clastic Facies Using Well-Y, Onshore Delta State, Nigeria. Journal of Geochemistry, 2014, 13p.
[105]. Özgül, N., 1976. Toroslar'm bazı temel jeoloji özellikleri. Bulletin of the Geological Society of Turkey, 19, 65-78.

[106]. Özgül, N., 1996. Bozkır-Hadim-Taşkent (Orta Toroslar'ın kuzey kesimi) dolayında yer alan tektono-stratigrafik birliklerin stratigrafisi. Maden Tetkik ve Arama Dergisi, 119 (119).
[107]. Parekh, P., Möller, P., Dulski, P., and Bausch, W., 1977. Distribution of trace elements between carbonate and non-carbonate phases of limestone. Earth and Planetary Science Letters, 34 (1), 39-50.
[108]. Peters, K., 1986. Guidelines for evaluating petroleum source rock using programmed pyrolysis. AAPG Bulletin, 70 (3), 318-329.
[109]. Peters, K., and Cassa, M., 1994. Applied Source Rock Geochemistry: Chapter 5: Part II. Essential Elements.
[110]. Peters, K., and Moldowan, J., 1993. The biomarker guide: interpreting molecular fossils in petroleum and ancient sediments.
[111]. Piepgras, D., and Jacobsen, S., 1992. The behavior of rare earth elements in seawater: Precise determination of variations in the North Pacific water column. Geochimica et Cosmochimica Acta, 56 (5), 1851-1862.
[112]. Piper, D., 1974. Rare earth elements in the sedimentary cycle: a summary. Chemical Geology, 14 (4), 285-304.
[113]. Rantitsch, G., Melcher, F., Meisel, T., and Rainer, T., 2003. Rare earth, major and trace elements in Jurassic manganese shales of the Northern Calcareous Alps: hydrothermal versus hydrogenous origin of stratiform manganese deposits. Mineralogy and Petrology, 77 (1-2), 109-127.
[114]. Roser, B., and Korsch, R., 1986. Determination of tectonic setting of sandstone-mudstone suites using content and ratio. The Journal of Geology, 94 (5), 635-650.
[115]. Roser, B., and Korsch, R., 1988. Provenance signatures of sandstone-mudstone suites determined using discriminant function analysis of major-element data. Chemical Geology, 67 (1-2), 119-139.
[116]. Sarı, A., 1994. Organic facies properties of sedimentary units of Mesozoic in Boyabat (Sinop) region, Northern Turkey. Geological Bulletin of Turkey, V. 37,(No. 2), 111 -118.
[117]. Sari, A., and Aliyev, S., 2006. Organic geochemical characteristics of the Paleocene–Eocene oil shales in the Nallıhan Region, Ankara, Turkey. Journal of Petroleum Science and Engineering, 53 (1), 123-134.
[118]. Sarı, A., and Bozkurt, S., 2012. Dağhacilar güneyi (Göynük/Bolu) bitümlü kayaçlarinin organik madde miktarlari ve hidrokarbon potansiyellerinin incelenmesi. Master thesis.
[119]. Sarı, A., Moradi, A. V., and Akkaya, P., 2015. Evaluation of source rock potential, matrix effect and applicability of gas oil ratio potential factor in Paleocene–Eocene bituminous shales of Çamalan Formation, Nallıhan–Turkey. Marine and Petroleum Geology, 67, 180-186.
[120]. Sarı, A., and Yarıcı, T., 2012. Investigation of organic matter amount and hydrocarbon potential of the bituminous rocks in the north of dağhacilar (Bolu,Turkey) area. Master thesis.
[121]. Scherer, M., and Seitz, H., 1980. Rare-earth element distribution in Holocene and Pleistocene corals and their redistribution during diagenesis. Chemical Geology, 28, 279-289.
[122]. Schieber, J., 1988. Redistribution of rare-earth elements during diagenesis of carbonate rocks from the mid-Proterozoic Newland Formation, Montana, USA. Chemical Geology, 69 (1-2), 111-126.
[123]. Shalaby, M., Hakimi, M., and Abdullah, W., 2011. Geochemical characteristics and hydrocarbon generation modeling of the Jurassic source rocks in the Shoushan Basin, north Western Desert, Egypt. Marine and Petroleum Geology, 28 (9), 1611-1624.
[124]. Sholkovitz, E., 1988. Rare earth elements in the sediments of the North Atlantic Ocean, Amazon Delta, and East China Sea; reinterpretation of terrigenous input patterns to the oceans. American Journal of Science, 288 (3), 236-281.
[125]. Sholkovitz, E., 1992. Chemical evolution of rare earth elements: fractionation between colloidal and solution phases of filtered river water. Earth and Planetary Science Letters, 114 (1), 77-84.
[126]. Singh, A., Tewari, V., Sial, A., Khanna, P., and Singh, N., 2016. Rare earth elements and stable isotope geochemistry of carbonates from the mélange zone of Manipur ophiolitic Complex, Indo-Myanmar Orogenic Belt, Northeast India. Carbonates and evaporites, 31 (2), 139-151.
[127]. Stach, E., 1982. Stach's textbook of coal petrology.
[128]. Tao, S., Shan, Y., Tang, D., Xu, H., Li, S., and Cui, Y., 2016. Mineralogy, major and trace element geochemistry of Shichanggou oil shales, Jimusaer, Southern Junggar Basin, China: Implications for provenance, palaeoenvironment and tectonic setting. Journal of Petroleum Science and Engineering, 146, 432-445.
[129]. Taylor, S., and McLennan, S., 1985. The continental crust: its composition and evolution.
[130]. Tissot, B., and Espitalie, J., 1975. L'evolution thermique de la matière organique des sédiments: applications d'une simulation mathématique. Potentiel pétrolier des bassins sédimentaires de reconstitution de l'histoire thermique des sédiments. Revue de l'Institut français du Pétrole, 30 (5), 743-778.
[131]. Tissot, B., Pelet, R., and Ungerer, P., 1987. Thermal history of sedimentary basins, maturation indices, and kinetics of oil and gas generation. AAPG Bulletin, 71 (12), 1445-1466.
[132]. Tissot, B., and Welte, D., 1984. Geochemical fossils and their significance in petroleum formation Petroleum Formation and Occurrence (pp. 93-130): Springer.
[133]. Tlig, S., and M'rabet, A., 1985. A comparative study of the rare earth element (REE) distributions within the Lower Cretaceous dolomites and limestones of Central Tunisia. Sedimentology, 32 (6), 897-907.
[134]. Toyoda, K., Nakamura, Y., and Masuda, A., 1990. Rare earth elements of Pacific pelagic sediments. Geochimica et Cosmochimica Acta, 54 (4), 1093-1103.
[135]. Tuchscherer, M., Reimold, W., Koeberl, C., and Gibson, R., 2005. Geochemical and petrographic characteristics of impactites and Cretaceous target rocks from the Yaxcopoil-1 borehole, Chicxulub impact structure, Mexico: Implications for target composition. Meteoritics & Planetary Science, 40 (9-10), 1513-1536.
[136]. Tucker, M., 1983. Diagenesis, geochemistry, and origin of a Precambrian dolomite: the Beck Spring Dolomite of eastern California. Journal of Sedimentary Research, 53 (4).
[137]. Turan, A., 2010. Beyreli (Hadim, Orta Toroslar) dolayinda allokton aladağ birliğinin stratigrafisi. J. Fac. Eng. Arch. Selcuk Univ, 25 (4).
[138]. Walker, J., Klein, C., Schidlowski, M., Schopf, J., Stevenson, D., and Walter, M., 1983. Environmental evolution of the Archean-early Proterozoic Earth. IN: Earth's earliest biosphere: Its origin and evolution (A84-43051 21-51). Princeton, NJ, Princeton University Press, 1983, p. 260-290., 1, 260-290.
[139]. Wang, Q., Zou, H., Hao, F., Zhu, Y., Zhou, X., Wang, Y., and Liu, J., 2014. Modeling hydrocarbon generation from the Paleogene source rocks in Liaodong Bay, Bohai Sea: A study on gas potential of oil-prone source rocks. Organic geochemistry, 76, 204-219.
[140]. Webb, G., and Kamber, B., 2000. Rare earth elements in Holocene reefal microbialites: a new shallow seawater proxy. Geochimica et Cosmochimica Acta, 64 (9), 1557-1565.
[141]. Wright, J., Schrader, H., and Holser, W., 1987. Paleoredox variations in ancient oceans recorded by rare earth elements in fossil apatite. Geochimica et Cosmochimica Acta, 51 (3), 631-644.

[142]. Zhao, Y, Zheng, Y., and Chen, F., 2009. Trace element and strontium isotope constraints on sedimentary environment of Ediacaran carbonates in southern Anhui, South China. Chemical Geology, 265 (3), 345-362.

Table. 1 Contents of Rock-Eval/TOC analysis and calculated parameters of the samples from the Early Permian Kuşakdağı Formation.

Sample NO.	TOC[a] (wt%)	S1[b] (mg HC[j]/g)	S2[c] (mg HC/g)	S3[d] (mg HC/g)	HI[e] (mg HC/g TOC)	OI[f] (mgCO2/g TOC)	PI[g] (S1/S1+S2)	Tmax[h] (°C)	PY[i] (PPM)
K1	0,42	0,02	0,33	0,31	79	74	0,05	449	350
K2	0,92	0,02	0,06	0,5	7	54	0,2	N/A[k]	80
K3	0,92	0,02	0,05	1,21	5	132	0,29	N/A[k]	70
K4	0,3	0,01	0,04	0,18	13	60	0,19	443	50
K5	4,15	0,03	0,49	4,19	12	101	0,05	534	520
K6	1,39	0,02	0,15	1,5	11	108	0,09	522	170
K7	0,3	0,01	0,07	0,21	23	70	0,16	508	80
K8	0,66	0,01	0,13	0,47	20	71	0,09	513	140
K9	2,46	0,02	0,34	2,17	14	88	0,07	520	360
K11	0,65	0,01	0,05	0,77	8	118	0,13	520	60
K12	0,22	0,01	0,05	0,18	23	82	0,14	483	60
K14	0,21	0,01	0,04	0,18	19	86	0,19	473	50
K15	0,16	0,01	0,03	0,22	19	138	0,18	479	40
K16	0,27	0,01	0,11	0,22	41	81	0,11	472	120
K17	0,17	0,01	0,07	0,2	41	118	0,14	483	80
K19	0,14	0,01	0,03	0,14	21	100	0,17	477	40
K20	0,13	0,01	0,03	0,09	23	69	0,19	476	40
K21	0,19	0,01	0,07	0,18	37	95	0,12	478	80
K26	0,17	0,01	0,04	0,2	24	118	0,13	478	50
K33	0,13	0,01	0,05	0,18	38	138	0,17	448	60

[a]TOC = Total organic carbon; [b]S1 = Free hydrocarbons; [c]S2 = Pyrolysable hydrocarbons;

[d]S3 = Carbon dioxide; [e]HI = Hydrogen index; [f]OI = Oxygen index; [g]PI = Productivity index;

[h]Tmax = Temperature of maximum S2; [i]PY = Potential yield; [j]HC = Hydrocarbon.

[k]N/A = Due to high PI values unsuitable Tmax values

Table 2. Identification of the source rock quality based on TOC and Rock- Eval pyrolysis data from (K. Peters, 1986).

Quality	TOC (wt.%)	S1 (mg. Hc./gm rock)	S2 (mg. Hc./gm rock)
Poor	0 to <0.5	0–0.5	0–2.5
Fair	0.5–1.0	0.5–1.0	2.5–5
Good	1–2	1–2	5–10
Very good	>2	>2	>10

Table 3. Determination of kerogen types according to S2/S3 parameters from (K. E. Peters and Cassa, 1994).

S2/S3	Kerogen Type
> 15	I
10-15	II
5-10	II/III
1-5	III
< 1	IV

Table 4. Kerogen and hydrocarbon types according to HI values From (K. E. Peters and Cassa, 1994) .

HI (mg HC/g Corg)	Kerogen type and HC type
<50	Type IV, little gas
50-200	Type III, gas
200-300	Type II-Tip III, oil and gas
300-600	Type II, oil
>600	Type I, oil

Table 5. Major oxide, total carbon (TOTC), total sulphur (TOTS), Loss On Ignition (LOI) contents (wt %) and clastic and carbonate ratios of the samples from the Kuşakdağı and Gökçepınar Formations.

SAMPLES	SiO_2	Al_2O_3	Fe_2O_3	MgO	CaO	Na_2O	K_2O	TiO_2	P_2O_5	MnO	Cr_2O_3	LOI	Total	Clastic	Carbonate	TOTC	TOTS
K1	3,96	0,38	0,21	0,66	52,28	0,05	0,04	0,02	0,01	0,01	0,002	42,2	99,84	4,86	95,14	12,66	0,08
K2	8,57	2,55	2,27	0,86	46,87	0,2	0,2	0,13	0,01	0,02	0,006	37,9	99,62	14,37	85,63	11,47	0,59
K3	***71,67***	***12,68***	***3,11***	***0,51***	***1,47***	***0,41***	***1,1***	***0,76***	***0,03***	***0,01***	***0,016***	***8,1***	***99,89***	***89,92***	***10,08***	***11,24***	***0,03***
K4	2,5	0,86	0,34	0,9	52,7	0,03	0,18	0,04	0,01	0,01	0,003	42,3	99,82	4,1	95,9	12,64	0,25
K5	***43,92***	***15,49***	***3,53***	***0,89***	***5,44***	***0,12***	***1,29***	***0,9***	***0,04***	***0,01***	***0,022***	***28,1***	***99,81***	***65,57***	***34,43***	***11,69***	***0,21***
K6	10,96	4,11	1,46	0,41	43,61	0,05	0,36	0,19	0,01	0,01	0,005	38,4	99,56	17,58	82,42	11,69	0,05
K7	4,47	1,22	0,53	0,59	51,15	0,03	0,1	0,06	0,01	0,01	0,002	41,6	99,74	6,66	93,34	12,52	0,07
K9	17,23	5,82	2,43	0,63	36,79	0,06	0,69	0,29	0,01	0,01	0,006	35,6	99,55	26,98	73,02	11,48	0,09
K11	***33,72***	***12,8***	***5,81***	***0,95***	***18,76***	***0,38***	***1,37***	***0,61***	***0,03***	***0,04***	***0,014***	***25,2***	***99,69***	***55,09***	***44,91***	***6,89***	***0,07***
K12	3,63	0,94	0,45	0,87	51,82	0,06	0,14	0,05	0,01	0,01	0,002	41,9	99,87	5,41	94,59	12,35	0,06
K15	3,38	0,65	0,26	0,79	52,46	0,01	0,1	0,03	0,01	0,01	0,002	42,2	99,94	4,55	95,45	12,48	0,02
K17	1,56	0,42	0,21	0,81	53,73	0,01	0,09	0,02	0,01	0,01	0,002	43,1	99,93	2,36	97,64	12,75	0,03
K20	0,71	0,29	0,17	0,84	54,05	0,01	0,08	0,01	0,01	0,01	0,002	43,8	99,93	1,31	98,69	13,07	0,03
K23	1,97	0,6	0,22	0,96	52,95	0,02	0,15	0,03	0,01	0,01	0,002	43	99,91	3,09	96,91	12,51	0,04
K26	1,07	0,32	0,19	0,72	54,04	0,02	0,07	0,02	0,01	0,01	0,002	43,5	99,92	1,74	98,26	12,66	0,03
K29	1,4	0,25	0,19	0,75	53,97	0,02	0,05	0,01	0,01	0,01	0,002	43,3	99,92	1,98	98,02	12,76	0,02
K32	2,42	0,5	0,25	0,78	53,25	0,01	0,11	0,02	0,01	0,01	0,002	42,5	99,91	3,47	96,53	12,58	0,03
K33	1,92	0,28	0,17	0,76	53,64	0,01	0,06	0,02	0,01	0,01	0,002	43,1	99,92	2,5	97,5	12,44	0,02
K37	2,45	0,47	0,16	0,89	53,04	0,02	0,1	0,02	0,01	0,01	0,002	42,7	99,92	3,37	96,63	12,45	0,03
K39	4,11	0,47	0,19	0,86	52,27	0,02	0,09	0,03	0,01	0,01	0,002	41,9	99,91	4,97	95,03	12,43	0,03
K40	5,36	0,59	0,42	0,73	51,78	0,02	0,09	0,06	0,01	0,01	0,002	40,8	99,91	6,69	93,31	12,01	0,28
K41	3,05	1,05	0,63	0,83	51,97	0,02	0,23	0,05	0,01	0,01	0,002	42,1	99,91	5,1	94,9	12,26	0,03
T1	1,72	0,55	1,38	5,34	47,15	0,02	0,1	0,03	0,01	0,01	0,002	43,6	99,86	3,91	96,09	12,78	0,03
T2	2,44	0,43	0,29	0,29	53,57	0,01	0,07	0,03	0,01	0,01	0,002	42,6	99,77	3,54	96,46	12,76	0,04
T3	1,62	0,52	1,2	4,59	48,43	0,02	0,09	0,03	0,01	0,01	0,002	43,4	99,86	3,58	96,42	12,79	0,03
T4	1,41	0,44	0,44	0,34	54,23	0,01	0,09	0,03	0,01	0,01	0,002	42,8	99,8	2,63	97,37	12,83	0,03
T5	3,84	1,06	0,57	0,33	52,17	0,01	0,18	0,07	0,01	0,01	0,002	41,6	99,8	5,9	94,1	12,03	0,02
T6	5,14	0,74	0,43	0,25	51,76	0,01	0,13	0,06	0,01	0,01	0,002	41,2	99,75	6,79	93,21	12,02	0,02
Avg,	8,79	2,37	0,98	1,00	46,62	0,06	0,26	0,13	0,01	0,01	0,004	39,59	99,83			12,15	0,08
ASC_a	64,21	17,02	6,71	2,7	3,44	1,44	3,58	0,72	0,19	0,65	-	-	-			-	-
$PAAS_b$	62,8	18,9	7,22	2,2	1,3	1,2	3,7	1	0,16	0,11	0,01	6					
$NASC_c$	64,8	16,9	5,66	2,86	3,63	1,14	3,97	0,7	0,13	0,06	-	-	-			-	-

The samples with bold color (K3, K5, K11) are in shale composition. The other ones are in limestone compositions.
a) From (Clarke, 1924)

b) From (Taylor and McLennan, 1985)

c) From (Gromet et al., 1984)

Table 6. Key major and trace element ratios for the samples from the Kuşakdağı and Gökçepınar Formations.

Sample	Al/(Al+Fe+Mn)	K_2O/Na_2O	Al_2O_3/TiO_2	Sr/Cu	Sr/Ba	V/V+Ni	LRE/HRE	ΣREE	Y/Ho	Eu/Eu* **a**	Eu/Eu* **b**	Ce/Ce* **a**	Ce/Ce* **b**	Ce anom **c**
K1	0,63	0,80	19,00	628,78	94,32	4,50	2,71	7,31	30,00	1,41	1,28	1,12	1,14	0,08
K2	0,53	1,00	19,62	998,79	82,25	10,30	5,71	93,29	26,86	1,07	0,97	0,97	0,99	-0,01
K3	0,80	2,68	16,68	23,22	2,93	4,40	6,42	176,17	26,90	0,86	0,78	1,06	1,08	0,01
K4	0,71	6,00	21,50	636,85	424,57	5,60	4,15	23,04	32,00	0,83	0,75	0,87	0,89	-0,07
K5	0,81	10,75	17,21	24,60	3,28	13,80	6,05	222,97	24,10	0,85	0,77	1,00	1,02	-0,02
K6	0,74	7,20	21,63	571,25	98,67	13,10	7,14	104,78	23,43	0,99	0,89	0,93	0,94	-0,03
K7	0,69	3,33	20,33	1025,58	278,37	4,40	4,51	24,01	33,33	1,03	0,93	0,96	0,98	-0,02
K9	0,70	11,50	20,07	369,39	86,86	18,00	8,70	107,54	22,58	0,98	0,88	0,97	0,99	-0,01
K11	0,69	3,61	20,98	93,02	20,19	36,70	5,84	258,28	25,31	1,04	0,95	0,84	0,86	-0,09
K12	0,67	2,33	18,80	160,84	136,72	4,60	3,78	40,30	31,58	1,04	0,94	0,89	0,90	-0,08
K15	0,71	10,00	21,67	160,90	45,97	4,10	3,82	13,22	27,14	1,27	1,13	0,87	0,88	-0,09
K17	0,66	9,00	21,00	274,15	89,10	3,30	3,10	10,87	63,33	0,95	0,84	1,04	1,05	-0,02
K20	0,62	8,00	29,00	347,25	208,35	2,90	3,46	9,37	37,50	1,04	0,91	1,03	1,05	0,00
K23	0,72	7,50	20,00	96,90	116,28	2,90	4,29	53,03	31,30	0,94	0,85	0,86	0,87	-0,09
K26	0,62	3,50	16,00	166,00	171,53	3,30	4,37	14,12	30,00	1,09	0,97	0,77	0,78	-0,14
K29	0,56	2,50	25,00	568,00	170,40	3,10	3,15	15,72	40,00	0,87	0,78	0,84	0,85	-0,11
K32	0,66	11,00	25,00	452,08	271,25	2,10	3,69	33,16	39,23	0,98	0,87	0,95	0,97	-0,05
K33	0,61	6,00	14,00	518,22	155,47	2,80	4,68	14,94	31,67	1,08	0,96	0,72	0,73	-0,22
K37	0,73	5,00	23,50	275,17	165,10	3,60	3,76	19,98	51,67	0,99	0,88	0,85	0,86	-0,10
K39	0,70	4,50	15,67	306,65	260,65	2,40	3,14	16,47	32,22	0,81	0,72	0,86	0,87	-0,12
K40	0,58	4,50	9,83	267,74	39,13	6,90	3,20	30,38	31,88	0,96	0,86	0,91	0,92	-0,08
K41	0,62	11,50	21,00	105,64	92,96	3,20	4,10	30,05	26,67	0,96	0,87	0,85	0,86	-0,11
T1	0,28	5,00	18,33	124,10	32,06	3,20	2,38	28,03	39,38	1,03	0,92	0,57	0,58	-0,29
T2	0,59	7,00	14,33	127,27	371,62	3,50	1,82	18,99	34,00	1,01	0,89	0,97	0,99	-0,03
T3	0,30	4,50	17,33	91,35	35,02	3,90	2,36	30,94	39,44	0,93	0,83	0,60	0,61	-0,26
T4	0,49	9,00	14,67	520,37	312,22	3,00	2,09	26,56	31,00	1,04	0,92	0,96	0,98	-0,01
T5	0,65	18,00	15,14	901,29	139,29	3,40	3,03	29,61	32,50	1,05	0,94	0,89	0,91	-0,06
T6	0,63	13,00	12,33	639,97	180,35	4,30	2,99	21,20	30,00	1,10	0,98	0,92	0,94	-0,04
Avg.	0,63	6,74	18,92	374,12	145,89	6,33	4,09	52,65	33,04	1,01	0,90	0,90	0,91	-0,07

a) normalized to PAAS from (Taylor and McLennan, 1985)

b) normalized to NASC from (Gromet et al., 1984)

c) normalized to chondrite from (Taylor and McLennan, 1985)

Table 7. Trace elements concentrations (ppm) of the samples from the Kuşakdağı and Gökçepınar Formations..

Sample	Sc	Cu	Pb	Zn	Ni	Ba	Co	Cs	Ga	Hf	Nb	Rb	Sr	Ta	Th	U	V	Zr
K1	1	1,8	8,2	10	3,5	12	0,3	0,6	0.5	0,1	0,3	1,5	1131,8	0,1	0,3	3,7	20	4,2
K2	3	2,8	6,8	12	9,3	34	2,6	1	1,6	0,8	2,9	7,8	2796,6	0,2	2,5	5,4	67	32,6
K3	8	8,7	22,7	6	3,4	69	1,7	6,9	17	4,2	17,2	49,6	202	1,2	10,6	3,1	157	155,6
K4	1	2	3,5	8	4,6	3	0,3	0,3	0,5	0,2	0,8	4,4	1273,7	0,1	0,6	5,1	26	8,8
K5	13	12,8	19,8	15	12,8	96	4,1	6,6	21,7	5,5	24,6	78,7	314,9	1,7	10,5	24	351	240,2
K6	3	5,7	6,2	16	12,1	33	3,4	1,1	3,6	1,3	5,8	17,4	3256,1	0,4	4	8	81	55,5
K7	1	1,9	2,6	7	3,4	7	0,9	0,1	0,5	0,4	1,5	4,5	1948,6	0,1	0,8	2,3	25	15,9
K9	4	8,7	9,1	24	17	37	6,4	2	5	2	8,6	32	3213,7	0,6	5,3	8,3	92	80,6
K11	11	16,5	16,7	62	35,7	76	14,8	6,3	15,5	4,3	17,7	70,2	1534,8	1,1	11,5	10,9	193	171,4
K12	1	5,1	2,6	4	3,6	6	0,7	0,3	0,5	0,5	1,3	6,1	820,3	0,1	1,1	1,8	14	18,3
K15	1	2	3	6	3,1	7	0,8	0,2	0,5	0,2	0,7	3,5	321,8	0,1	0,4	1,9	27	8,6
K17	1	1,3	2,2	5	2,3	4	0,8	0,3	0,5	0,2	0,4	2,5	356,4	0,1	0,3	1,7	16	6,5
K20	1	1,2	1,8	5	1,9	2	0,2	0,1	0,5	0,2	0,1	1,6	416,7	0,1	0,2	1,9	19	4,9
K23	1	4,8	6,4	5	1,9	4	0,4	0,4	0,5	0,2	0,6	4,8	465,1	0,1	0,8	1,7	23	7,9
K26	1	3,1	3,1	5	2,3	3	0,6	0,2	0,5	0,1	0,6	1,7	514,6	0,1	0,2	2,2	12	5,1
K29	1	0,9	2,8	3	2,1	3	0,2	0,1	0,5	0,1	0,3	1,2	511,2	0,1	0,2	2	11	4,8
K32	1	1,2	2,1	4	1,1	2	0,2	0,4	0,5	0,1	0,4	3,3	542,5	0,1	0,4	1,2	13	6,1
K33	1	0,9	2,4	3	1,8	3	0,2	0,2	0,5	0,1	0,2	1,8	466,4	0,1	0,3	1,5	18	4,7
K37	1	1,8	1,9	4	2,6	3	0,5	0,1	0,5	0,2	0,4	3,3	495,3	0,1	0,7	2,1	9	8,2
K39	1	1,7	2,2	3	1,4	2	0,3	0,1	0,5	0,6	0,7	2,7	521,3	0,1	0,4	2,4	18	28,3
K40	1	1,9	3,3	7	5,9	13	3,3	0,1	0,5	1,3	1,6	2,7	508,7	0,1	1,1	3	30	60,3
K41	1	4,4	5,7	7	2,2	5	0,6	0,7	0,5	0,3	1	7,4	464,8	0,1	0,7	1,7	22	12,4
T1	1	3,1	3,3	5	2,2	12	0,6	0,1	0,5	0,3	0,4	2,9	384,7	0,1	0,3	0,5	10	10,4
T2	1	14,6	40,8	5	2,5	5	0,2	0,1	0,5	0,3	0,3	1,6	1858,1	0,1	0,4	0,3	8	10
T3	1	4,6	4,1	6	2,9	12	0,8	0,1	0,5	0,1	0,3	2,6	420,2	0,1	0,3	0,5	9	8
T4	1	3	4,3	4	2	5	0,5	0,1	0,5	0,2	0,3	2,2	1561,1	0,1	0,5	0,3	15	9,4
T5	1	1,7	3,1	4	2,4	11	1,2	0,3	0,5	0,5	1,2	5,6	1532,2	0,1	0,9	0,5	12	21
T6	1	3,1	2,7	3	3,3	11	0,7	0,1	0,5	0,5	0,7	3,5	1983,9	0,1	0,7	0,4	10	18,7
Avg.	2,3	4,3	6,9	8,9	5,3	17,1	1,7	1,0	2,8	0,9	3,2	11,7	1064,9	0,3	2,0	3,5	46,7	36,4
$PAAS_a$	16	50	20	85	55	650	23	15	20	5	19	160	200	1,12	14,6	3,1	150	210
NASC	$14,9_b$	45_c	20_d	$2,7_e$	58_b	636_b	$25,7_b$	$5,16_b$	-	$6,3_b$	13_d	125_b	142_b	$1,12_b$	$12,3_b$	$2,66_b$	130_c	200_b

$PAAS_a$ from (Taylor and McLennan, 1985)

$NASC_b$ from (Gromet et al., 1984)

$NASC_c$ from (Jarrar et al., 2000)

$NASC_d$ from (Condie, 1993)

$NASC_e$ from (Morgan et al., 1978)

Table 8. Rare earth element concentrations (ppm) of the samples from the Kuşakdağı and Gökçepınar Formations..

Sample	La	Ce	Pr	Nd	Sm	Eu	Gd	Tb	Dy	Y	Ho	Er	Tm	Yb	Lu	ΣREE	ΣLREE	ΣHREE
K1	1,1	2,7	0,28	0,8	0,21	0,06	0,19	0,03	0,18	1,5	0,05	0,11	0,01	0,08	0,01	7,31	5,34	1,97
K2	17,2	35,8	4,2	15,9	3,07	0,64	2,58	0,34	1,93	9,4	0,35	0,88	0,12	0,78	0,1	93,29	79,39	13,9
K3	36,8	77,1	7,58	24,8	3,25	0,51	2,4	0,39	2,67	15,6	0,58	1,95	0,29	1,95	0,3	176,17	152,44	23,73
K4	4,5	8	0,99	3,6	0,7	0,12	0,66	0,07	0,53	3,2	0,1	0,28	0,03	0,23	0,03	23,04	18,57	4,47
K5	47,7	93,5	9,67	32,2	4,43	0,68	3,18	0,54	3,95	20	0,83	2,72	0,4	2,75	0,42	222,97	191,36	31,61
K6	20,1	40,5	5,06	19,1	3,76	0,67	2,72	0,39	2,09	8,2	0,35	0,86	0,12	0,76	0,1	104,78	91,91	12,87
K7	4,4	8,9	1,03	3,8	0,68	0,15	0,69	0,09	0,59	3	0,09	0,27	0,03	0,26	0,03	24,01	19,65	4,36
K9	20,8	44,2	5,27	19,8	3,43	0,59	2,36	0,32	1,71	7	0,31	0,78	0,11	0,76	0,1	107,54	96,45	11,09
K11	53,4	92,3	11,9	45,1	8,76	1,77	7,28	1	5,24	24,8	0,98	2,58	0,37	2,47	0,33	258,28	220,51	37,77
K12	8	13,6	1,56	5,8	1,33	0,29	1,29	0,18	1,01	6	0,19	0,49	0,07	0,44	0,05	40,3	31,87	8,43
K15	2,7	4,5	0,52	2	0,31	0,09	0,36	0,05	0,37	1,9	0,07	0,17	0,02	0,15	0,01	13,22	10,48	2,74
K17	2	3,9	0,37	1,4	0,22	0,05	0,28	0,04	0,34	1,9	0,03	0,16	0,01	0,15	0,02	10,87	8,22	2,65
K20	1,7	3,5	0,36	1,2	0,19	0,05	0,27	0,04	0,28	1,5	0,04	0,13	0,01	0,09	0,01	9,37	7,27	2,1
K23	10,8	18,2	2,19	8,4	1,64	0,31	1,47	0,21	1,18	7,2	0,23	0,61	0,08	0,44	0,07	53,03	43,01	10,02
K26	3,2	4,7	0,62	2,1	0,36	0,09	0,42	0,05	0,33	1,8	0,06	0,21	0,02	0,15	0,01	14,12	11,49	2,63
K29	3,3	5,1	0,58	2	0,4	0,08	0,47	0,06	0,41	2,8	0,07	0,22	0,03	0,17	0,03	15,72	11,93	3,79
K32	6,1	11,5	1,27	5,2	0,81	0,19	1,02	0,14	0,82	5,1	0,13	0,42	0,05	0,37	0,04	33,16	26,09	7,07
K33	4,2	4,9	0,53	1,9	0,32	0,08	0,38	0,05	0,34	1,9	0,06	0,13	0,01	0,13	0,01	14,94	12,31	2,63
K37	4	6,7	0,82	3,1	0,49	0,11	0,56	0,07	0,47	3,1	0,06	0,26	0,03	0,19	0,02	19,98	15,78	4,2
K39	3,3	5,2	0,58	2,4	0,42	0,08	0,51	0,06	0,44	2,9	0,09	0,21	0,03	0,22	0,03	16,47	12,49	3,98
K40	5,8	10	1,11	4,4	0,8	0,17	0,87	0,13	0,82	5,1	0,16	0,48	0,07	0,41	0,06	30,38	23,15	7,23
K41	6,1	10	1,21	4,9	0,9	0,18	0,87	0,13	0,67	4	0,15	0,44	0,04	0,42	0,04	30,05	24,16	5,89
T1	5,9	6,3	1,09	4,3	0,87	0,21	1,06	0,14	0,82	6,3	0,16	0,46	0,05	0,33	0,04	28,03	19,73	8,3
T2	2,5	5,1	0,59	2,6	0,58	0,14	0,74	0,11	0,64	5,1	0,15	0,37	0,05	0,28	0,04	18,99	12,25	6,74
T3	6,2	7,1	1,18	5	0,94	0,2	1,1	0,15	0,92	7,1	0,18	0,46	0,05	0,32	0,04	30,94	21,72	9,22
T4	3,6	7,7	0,95	3,7	0,79	0,2	1,03	0,15	0,97	6,2	0,2	0,54	0,07	0,39	0,07	26,56	17,97	8,59
T5	4,9	9,2	1,16	4,8	0,93	0,22	1,05	0,15	0,87	5,2	0,16	0,47	0,06	0,39	0,05	29,61	22,26	7,35
T6	3,4	6,8	0,85	3,3	0,62	0,16	0,76	0,11	0,71	3,6	0,12	0,39	0,04	0,31	0,03	21,2	15,89	5,31
Avg.	10,49	19,54	2,27	8,34	1,47	0,29	1,31	0,19	1,12	6,12	0,21	0,61	0,08	0,55	0,07	52,65	43,70	8,95
$PAAS_a$	38,2	79,6	8,83	33,9	5,55	1,08	4,66	0,77	4,68	27	0,99	2,85	0,41	2,82	0,43			
NASC	$31,1_b$	$66,7_b$	$7,9_c$	$27,4_b$	$5,59_b$	$1,18_b$	$4,55_b$	$0,85_b$	$3,51_b$	27_d	$1,04_c$	$1,93_b$	$0,5_c$	$3,06_b$	$0,456_b$			

$PAAS_a$ from (Taylor and McLennan, 1985)

$NASC_b$ from (Gromet et al., 1984)

$NASC_c$ from (Haskin et al., 1968)

$NASC_d$ from (Jarrar et al., 2000)

Table 9. Pearson correlation coefficients among major, trace, and rare earth elements of the samples from the Kuşakdağı and Gökçepınar Formations.

	SiO_2	Al_2O_3	Fe_2O_3	MgO	CaO	Na_2O	K_2O	TiO_2	P_2O_5	MnO	LOI	TOTC	Cu	Pb	Ni	Ba	Nb	Rb	Sr	U	V	Zr	Ce	Eu	ΣREE
SiO_2	1,0																								
Al_2O_3	0,9	1,0																							
Fe_2O_3	0,8	0,9	1,0																						
MgO	-0,1	-0,1	0,1	1,0																					
CaO	-1,0	-1,0	-0,9	0,0	1,0																				
Na_2O	0,9	0,8	0,8	-0,1	-0,8	1,0																			
K_2O	0,9	1,0	0,9	-0,1	-1,0	0,8	1,0																		
TiO_2	0,9	1,0	0,9	-0,1	-1,0	0,8	1,0	1,0																	
P_2O_5	0,9	1,0	0,8	-0,1	-0,9	0,7	0,9	1,0	1,0																
MnO	0,3	0,5	0,7	0,0	-0,4	0,7	0,5	0,4	0,4	1,0															
LOI	-1,0	-0,9	-0,8	0,1	0,9	-0,9	-0,9	-0,9	-0,8	-0,4	1,0														
TOTC	-0,6	-0,7	-0,9	0,1	0,6	-0,8	-0,8	-0,6	-0,6	-0,9	0,6	1,0													
Cu	0,6	0,7	0,8	-0,1	-0,7	0,6	0,8	0,7	0,7	0,5	-0,6	-0,7	1,0												
Pb	0,5	0,5	0,4	-0,2	-0,5	0,5	0,5	0,5	0,5	0,2	-0,5	-0,3	0,8	1,0											
Ni	0,5	0,7	0,9	-0,1	-0,6	0,6	0,8	0,6	0,6	0,8	-0,5	-0,9	0,7	0,3	1,0										
Ba	0,9	1,0	0,9	0,0	-1,0	0,8	1,0	1,0	0,9	0,5	-0,8	-0,7	0,7	0,5	0,7	1,0									
Nb	0,9	1,0	0,9	-0,1	-1,0	0,8	1,0	1,0	1,0	0,4	-0,9	-0,7	0,7	0,5	0,7	1,0	1,0								
Rb	0,9	1,0	0,9	-0,1	-0,9	0,8	1,0	1,0	0,9	0,5	-0,8	-0,7	0,8	0,5	0,8	1,0	1,0	1,0							
Sr	0,0	0,1	0,2	-0,3	0,0	0,1	0,1	0,0	-0,2	0,2	0,0	-0,3	0,2	0,2	0,4	0,2	0,1	0,1	1,0						
U	0,6	0,8	0,7	-0,1	-0,7	0,4	0,8	0,8	0,8	0,3	-0,5	-0,5	0,6	0,3	0,6	0,8	0,8	0,8	0,2	1,0					
V	0,8	1,0	0,8	-0,1	-0,9	0,6	0,9	1,0	0,9	0,4	-0,7	-0,6	0,7	0,5	0,6	1,0	1,0	1,0	0,1	0,9	1,0				
Zr	0,9	1,0	0,9	-0,1	-0,9	0,7	1,0	1,0	0,9	0,4	-0,8	-0,7	0,7	0,5	0,7	1,0	1,0	1,0	0,0	0,8	1,0	1,0			
Ce	0,9	1,0	0,9	-0,1	-0,9	0,8	1,0	1,0	0,9	0,6	-0,9	-0,8	0,8	0,5	0,8	1,0	1,0	1,0	0,2	0,8	0,9	1,0	1,0		
Eu	0,6	0,8	0,9	0,0	-0,7	0,8	0,8	0,7	0,6	0,9	-0,6	-0,9	0,7	0,4	0,9	0,8	0,7	0,8	0,4	0,6	0,7	0,7	0,9	1,0	
ΣREE	0,8	1,0	1,0	-0,1	-0,9	0,8	1,0	0,9	0,9	0,6	-0,8	-0,8	0,8	0,5	0,8	1,0	1,0	1,0	0,2	0,8	0,9	0,9	1,0	0,9	1

Figure List:

Fig. 1 Location map of the study area.

Fig. 2 Simplified geological map of the Beyreli (Hadim-Konya) area, southern Turkey (modified from Turan, 2010).

Fig. 3 Generalized Stratigraphic columnar section of the study area (modified from Turan, 2010).

Fig. 4 Microscopic images of the shale and limestone samples from the Kuşakdağı Formation a- ***Hemigordius* sp.,** b- ***Mizzia* sp.,** c- ***Climacammina*** sp., d- ***Frondinodosaria*** sp., e- ***Hexagonaria*** sp., f- ***Globivalvulina* sp**.

Fig. 5 Sample locations on the stratigraphic section of the Kuşakdağı Formation.

Fig. 6. a) Plot diagrams of HI (mg HC/g TOC) versus TOC (wt.%) of the sample groups, indicating an poor potential for generating gas (from Jackson et al., 1985); b) Distribution of the carbonate samples on the S2 versus TOC plot diagram (from Dembicki Jr, 2009).

Fig. 7. a) A plot of HI versus OI of the samples from the Kuşakdağı Formation (from B. P. Tissot and Welte, 1984); b) Plot of Hydrogen Index (HI) versus (Rock-Eval) Tmax values for the samples analyzed showing kerogen quality and thermal maturity stages (from Espitalié et al., 1977).

Fig. 8. Provenance discrimination diagram for the Carbonate samples after Roser and Korsch (1988); Discriminant function 1 = (–1.773 TiO_2 + 0.607 Al_2O_3 + 0.76 Fe_2O_3 (total) – 1.5 MgO + 0.616 CaO + 0.509 Na_2O – 1.224 K_2O – 9.09); Discriminant function 2 = (0.445 TiO_2 + 0.07 Al_2O_3 – 0.25 Fe_2O_3 (total) –1.142 MgO + 0.438 CaO + 1.475 Na_2O + 1.426 K_2O – 6.861).

Fig. 9. PAAS-normalized major oxide patterns of the sample groups from the Kuşakdağı and Gökçepınar Formations.

Fig. 10. Composition of the sample groups from the Kuşakdağı and Gökçepınar Formations on the Na_2O/Al_2O_3 vs. K_2O/Al_2O_3 discrimination diagram (from Garrels, 1971).

Fig. 11. PAAS-normalized trace element patterns of the sample groups from the Kuşakdağı and Gökçepınar Formations.

Fig. 12. Plot of the sample groups from the Kuşakdağı and Gökçepınar Formations on the tectonic discrimination diagrams Th-Sc-Zr/10 and Th-Co-Zr/10 (after Bhatia and Crook, 1986). A. Oceanic island arc. B. Continental island arc. C. Active continental margins. D. Passive continental margins.

Fig. 13. Plot of the sample groups from the Kuşakdağı and Gökçepınar Formations on the Th/Sc versus Zr/Sc diagram (after S. McLennan et al., 1993).

Fig. 14. PAAS normalized REE patterns of the sample groups from the Kuşakdağı and Gökçepınar Formations.

Fig. 15. NASC normalized REE patterns of the sample groups from the Kuşakdağı and Gökçepınar Formations.

Fig. 16. Plot of Ce anomaly versus Nd concentrations; the dividing line between Anoxic and oxic is after (Wright et al., 1987).

Fig. 17. Hf–La/Th diagrams after (Floyd and Leveridge, 1987) of the sample groups from the Kuşakdağı and Gökçepınar Formations.
Fig. 18. Bivariate plots of the sample groups from the Kuşakdağı and Gökçepınar Formations a) CaO vs. SiO2, b) CaO vs. Al_2O_3, c) CaO vs. Fe_2O_3, d) CaO vs. TiO_2, e) CaO vs. K_2O, f) CaO vs. Cr_2O_3, g) CaO vs. Na_2O, h). CaO vs. P_2O_5.
Fig. 19., d) SiO_2 vs. TiO_2, e) TiO_2 vs. Al_2O_3, f) TiO_2 vs. Fe_2O_3, g) CaO vs. MgO, h) CaO vs. MnO.
Fig. 20. Bivariate plots of the sample groups Bivariate plots of the sample groups from the Kuşakdağı and Gökçepınar Formations. a) SiO_2 vs. Al_2O_3, b) SiO_2 vs. Fe_2O_3, c) SiO_2 vs. K_2O from the Kuşakdağı and Gökçepınar Formations. a) SiO_2+Al_2O_3+Fe_2O_3+Na_2O +K_2O+TiO_2 vs. Clastic %, b) CaO vs. Clastic%, c. LOI vs. Clastic%, d) ΣREE vs. Al_2O_3, e) ΣREE vs. CaO, f) Ce/Ce* vs. MnO, g) Ce/Ce* vs. Fe_2O_3, h) Ce/Ce* vs. Pb.
Fig. 21. Bivariate plots of the sample groups from the Kuşakdağı and Gökçepınar Formations. a) Ce/Ce* vs. U, b) Ce/Ce* vs. CaO, c) Ce/Ce* vs. SiO_2, d) Ce/Ce* vs. Zr.
Fig. 22. Bivariate plots of the sample groups from the Kuşakdağı and Gökçepınar Formations. a) Eu vs. Al_2O_3, b) Eu/Eu* vs. Zr, c) Eu/Eu* vs. Y, d) Eu/Eu* vs. Th, e) Eu/Eu* vs. Hf.
Fig. 23. Bivariate plots of the sample groups from the Kuşakdağı and Gökçepınar Formations. a) Al_2O_3 vs. Th, b) Al_2O_3 vs. Sc.

Fig. 1 Location map of the study area.

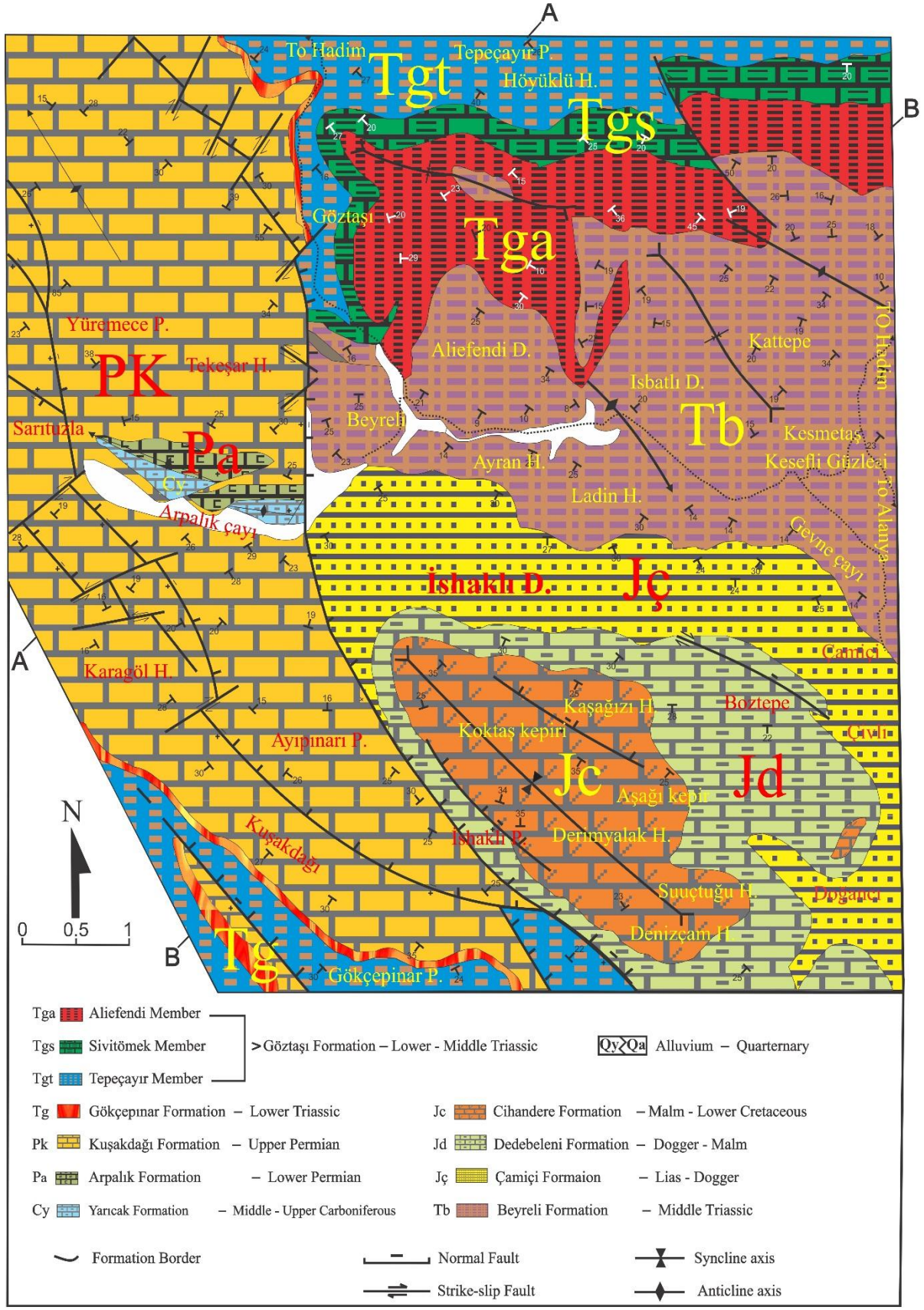

Fig. 2 Simplified geological map of the Beyreli (Hadim-Konya) area, southern Turkey (modified from Turan, 2010).

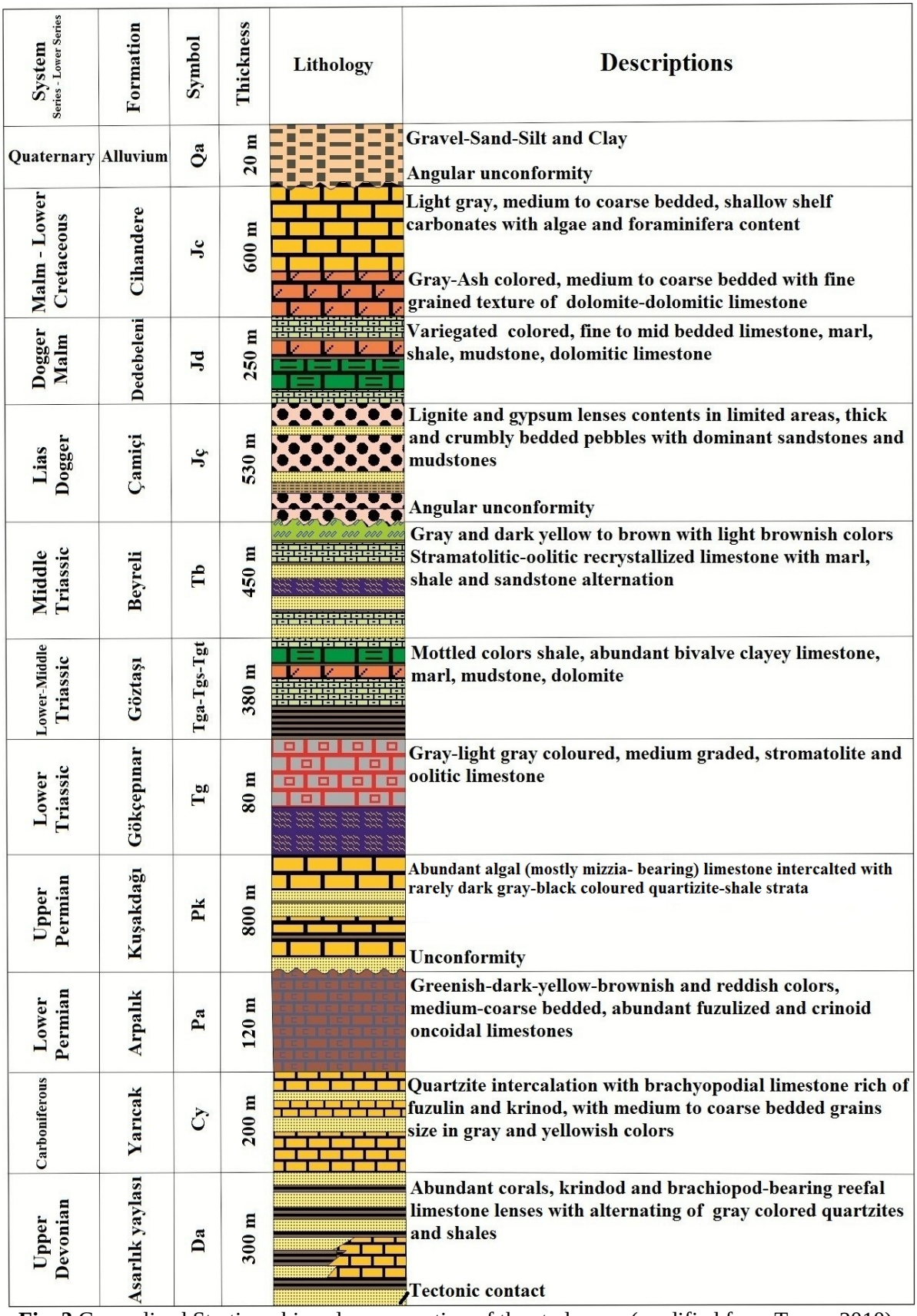

Fig. 3 Generalized Stratigraphic columnar section of the study area (modified from Turan, 2010).

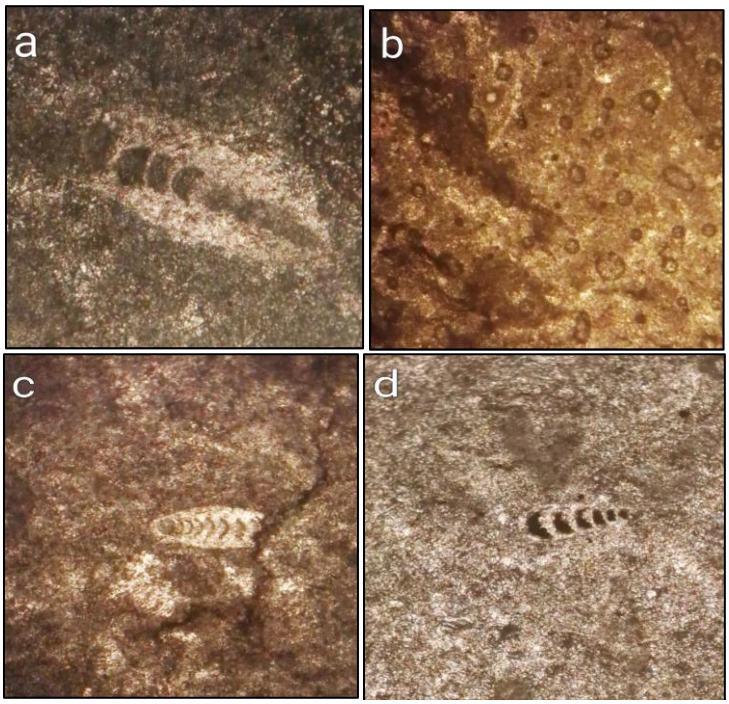

Fig. 4 Microscopic images of the shale and limestone samples from the Kuşakdağı Formation a- ***Hemigordius*** sp**.,** b- ***Mizzia*** sp**.,** c- ***Climacammina*** sp., d- ***Frondinodosaria*** sp., e- ***Hexagonaria*** sp., f- ***Globivalvulina*** sp.

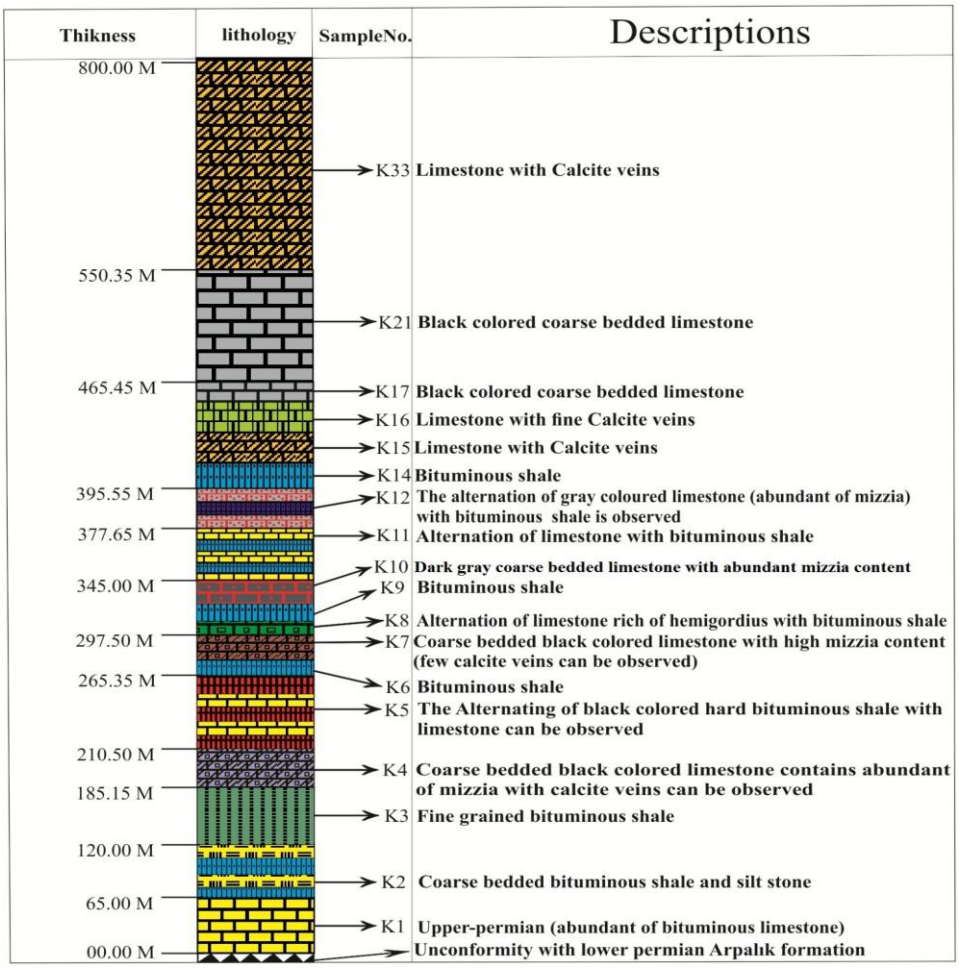

Fig. 5 Sample locations on the stratigraphic section of the Kuşakdağı Formation.

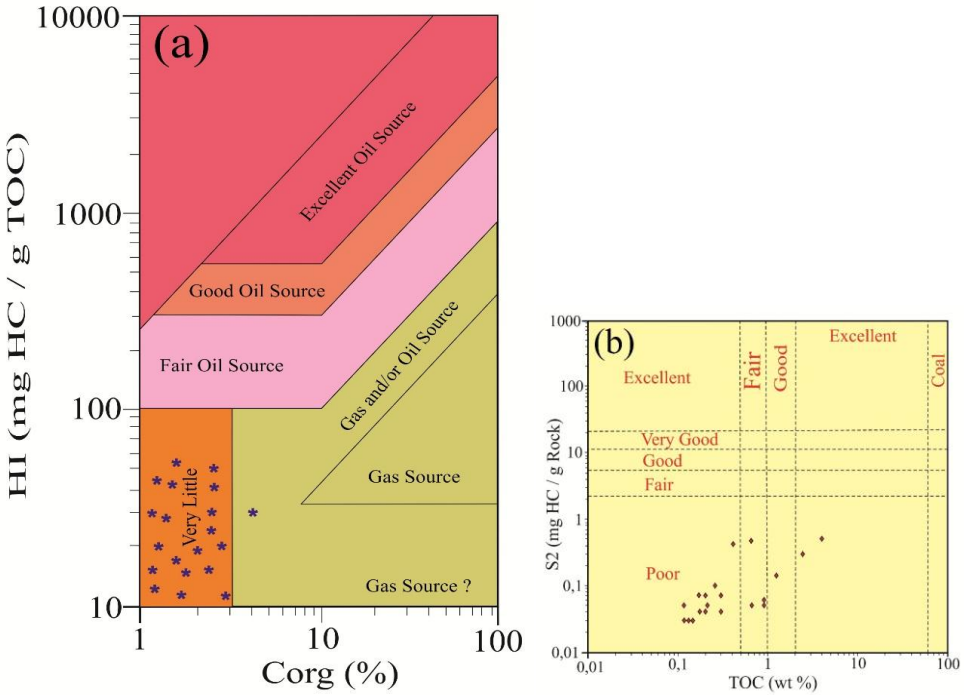

Fig. 6. a) Plot diagrams of HI (mg HC/g TOC) versus TOC (wt.%) of the sample groups, indicating an poor potential for generating gas (from Jackson et al., 1985); b) Distribution of the carbonate samples on the S2 versus TOC plot diagram (from Dembicki Jr, 2009).

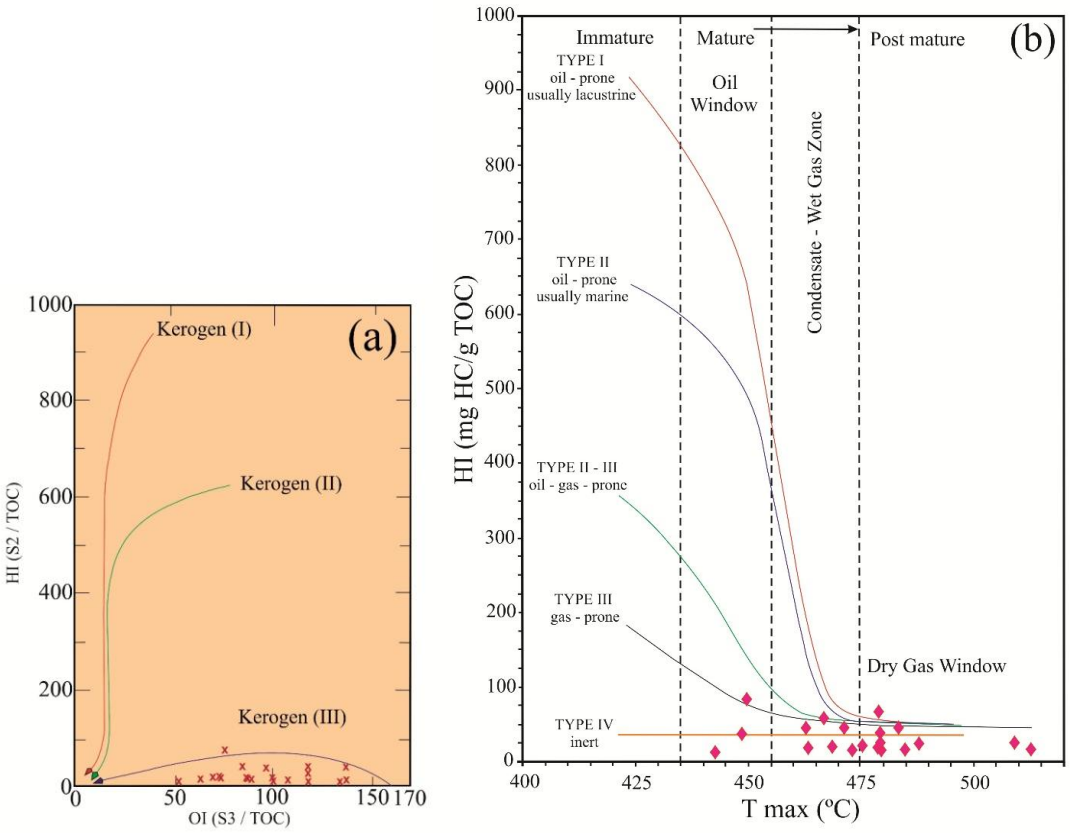

Fig. 7. a) A plot of HI versus OI of the samples from the Kuşakdağı Formation (from B. P. Tissot and Welte, 1984); b) Plot of Hydrogen Index (HI) versus (Rock-Eval) Tmax values for the samples analyzed showing kerogen quality and thermal maturity stages (from Espitalié et al., 1977).

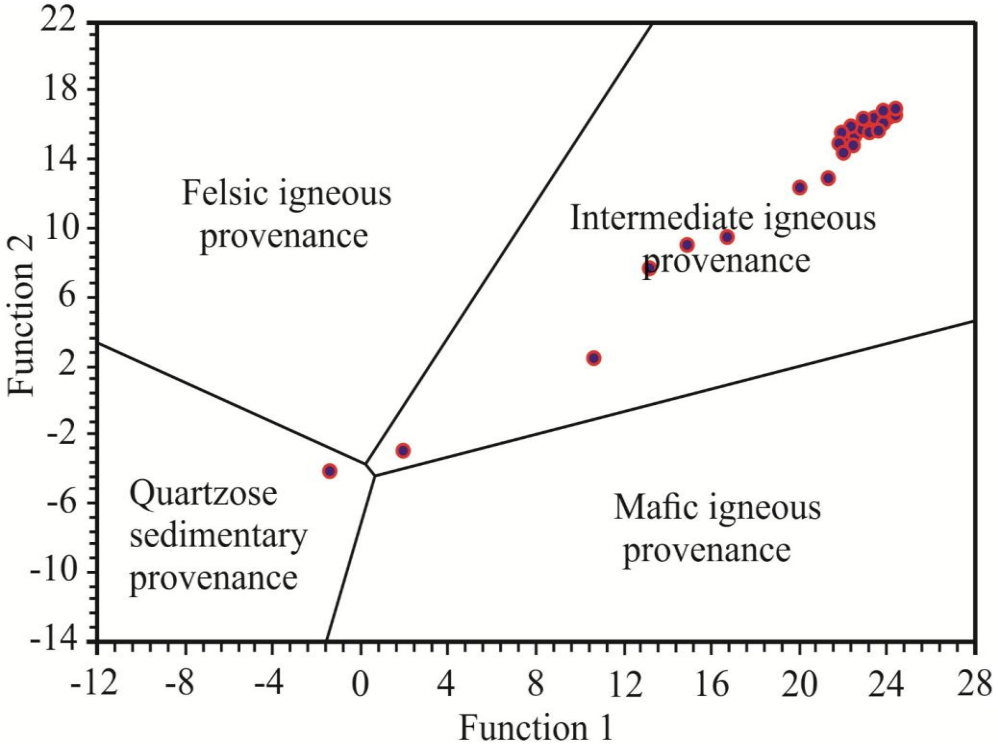

Fig. 8. Provenance discrimination diagram for the Carbonate samples after Roser and Korsch (1988); Discriminant function 1 = (–1.773 TiO_2 + 0.607 Al_2O_3 + 0.76 Fe_2O_3 (total) – 1.5 MgO + 0.616 CaO + 0.509 Na_2O – 1.224 K_2O – 9.09); Discriminant function 2 = (0.445 TiO_2 + 0.07 Al_2O_3 – 0.25 Fe_2O_3 (total) –1.142 MgO + 0.438 CaO + 1.475 Na_2O + 1.426 K_2O – 6.861).

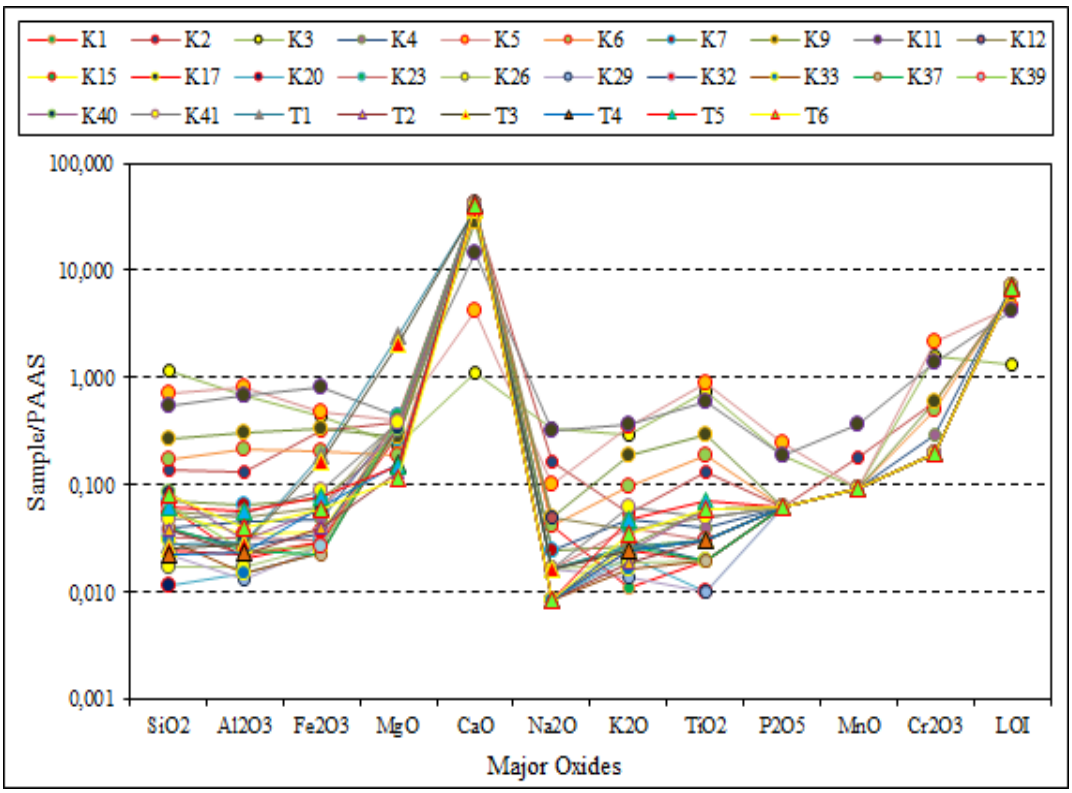

Fig. 9. PAAS-normalized major oxide patterns of the sample groups from the Kuşakdağı and Gökçepınar Formations.

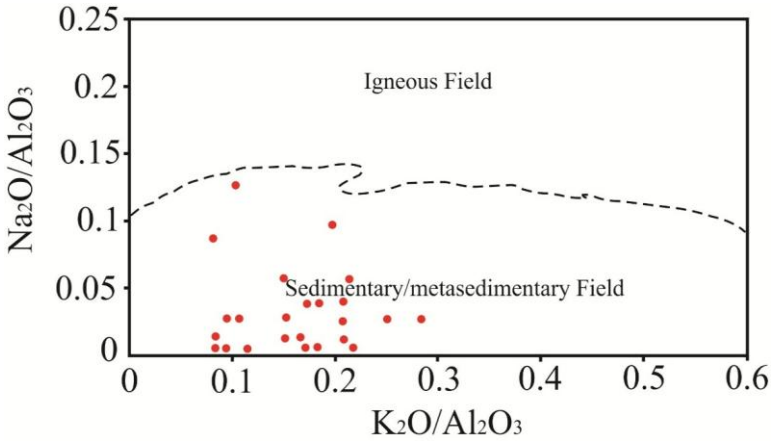

Fig. 10. Composition of the sample groups from the Kuşakdağı and Gökçepınar Formations on the Na_2O/Al_2O_3 vs. K_2O/Al_2O_3 discrimination diagram (from Garrels, 1971).

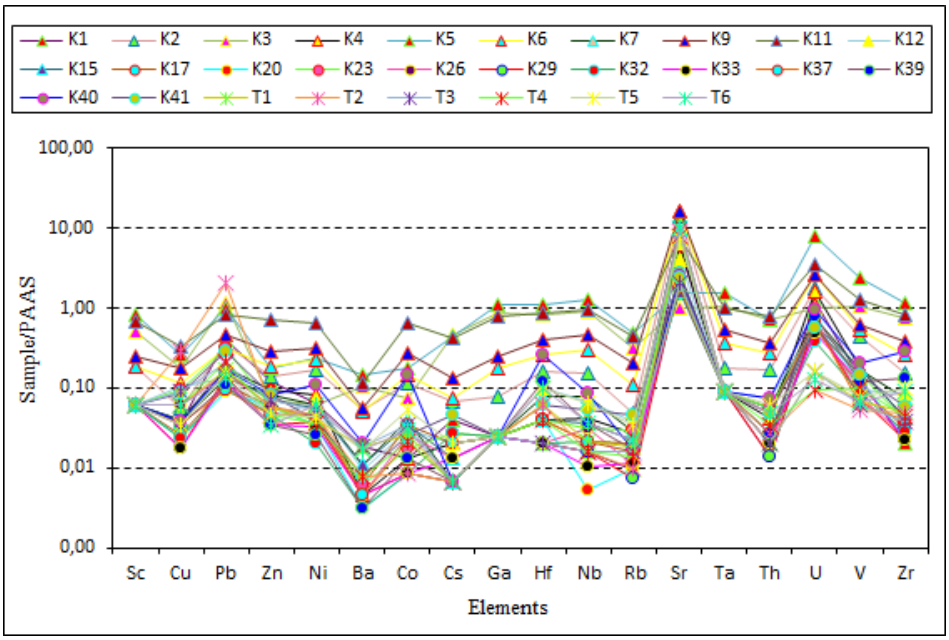

Fig. 11. PAAS-normalized trace element patterns of the sample groups from the Kuşakdağı and Gökçepınar Formations.

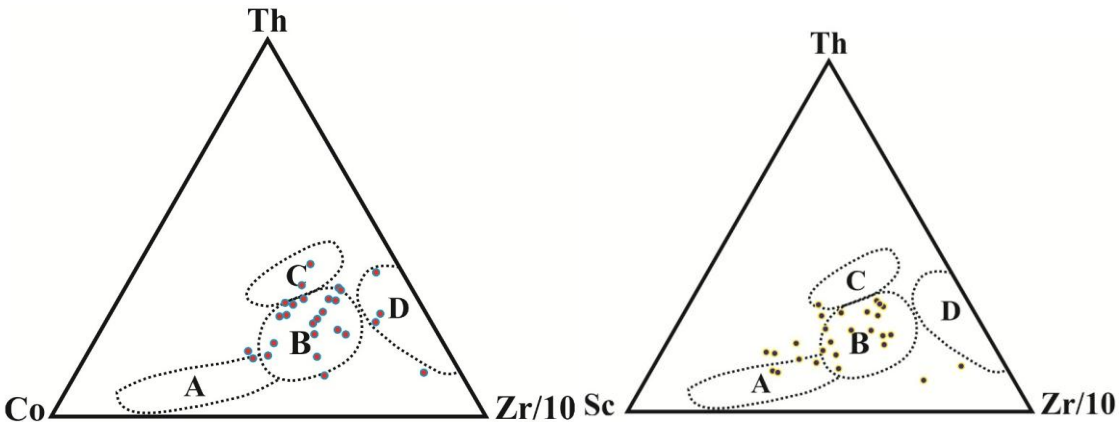

Fig. 12. Plot of the sample groups from the Kuşakdağı and Gökçepınar Formations on the tectonic discrimination diagrams Th-Sc-Zr/10 and Th-Co-Zr/10 (after Bhatia and Crook, 1986). A. Oceanic island arc. B. Continental island arc. C. Active continental margins. D. Passive continental margins

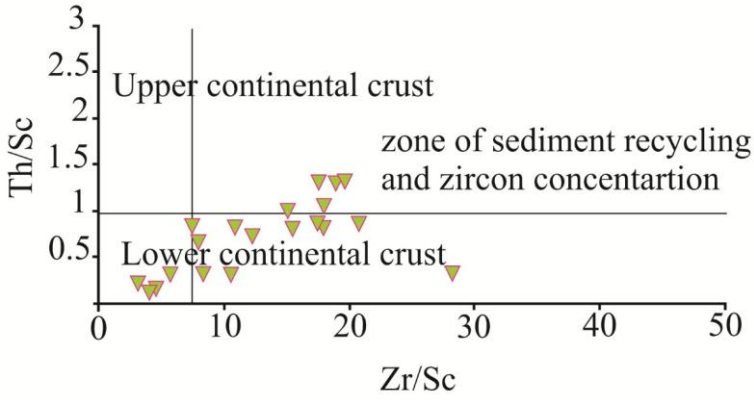

Fig. 13. Plot of the sample groups from the Kuşakdağı and Gökçepınar Formations on the Th/Sc versus Zr/Sc diagram (after S. McLennan et al., 1993).

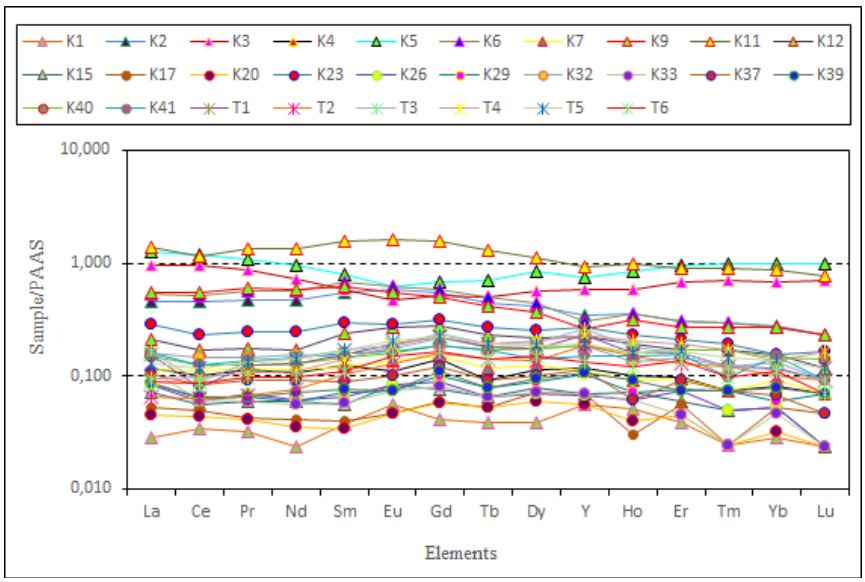

Fig. 14. PAAS normalized REE patterns of the sample groups from the Kuşakdağı and Gökçepınar Formations.

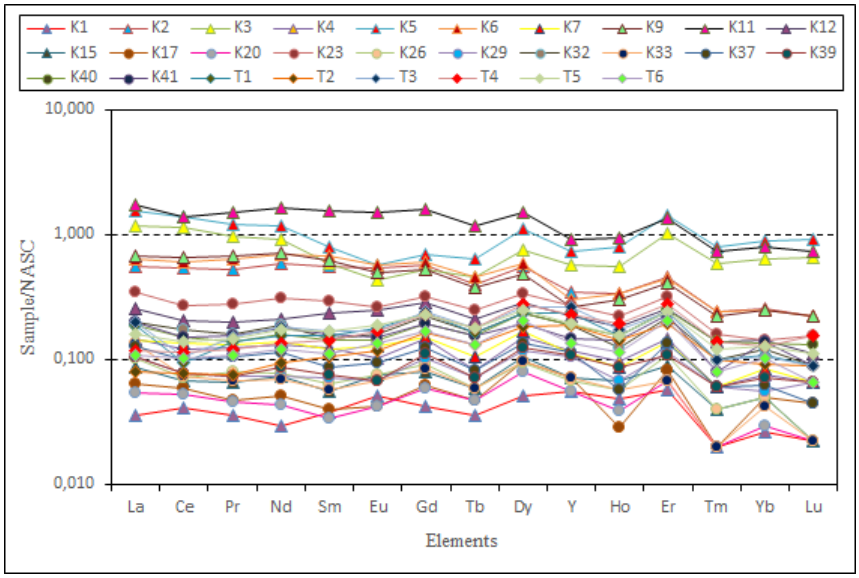

Fig. 15. NASC normalized REE patterns of the sample groups from the Kuşakdağı and Gökçepınar Formations.

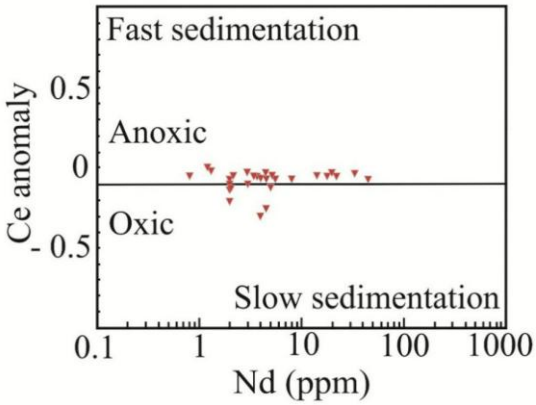

Fig. 16. Plot of Ce anomaly versus Nd concentrations; the dividing line between Anoxic and oxic is after (Wright et al., 1987).

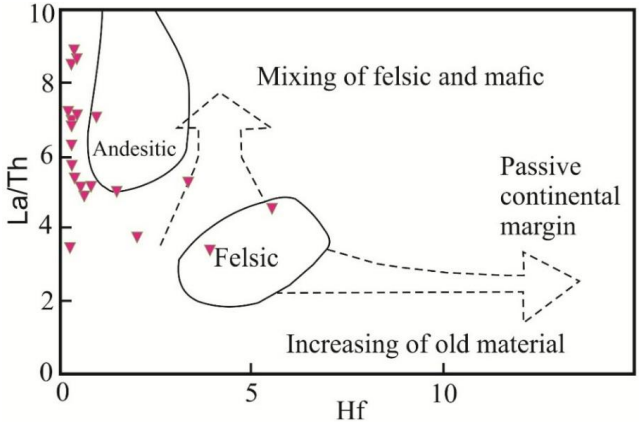

Fig. 17. Hf–La/Th diagrams after (Floyd and Leveridge, 1987) of the sample groups from the Kuşakdağı and Gökçepınar Formations.

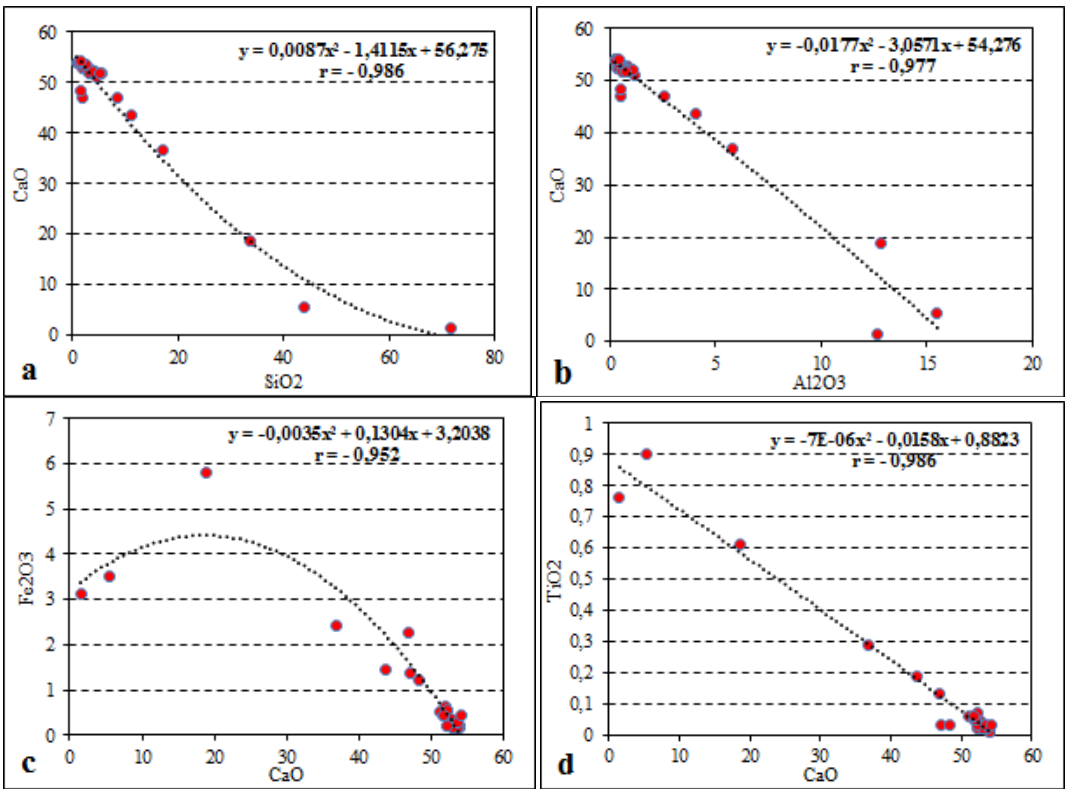

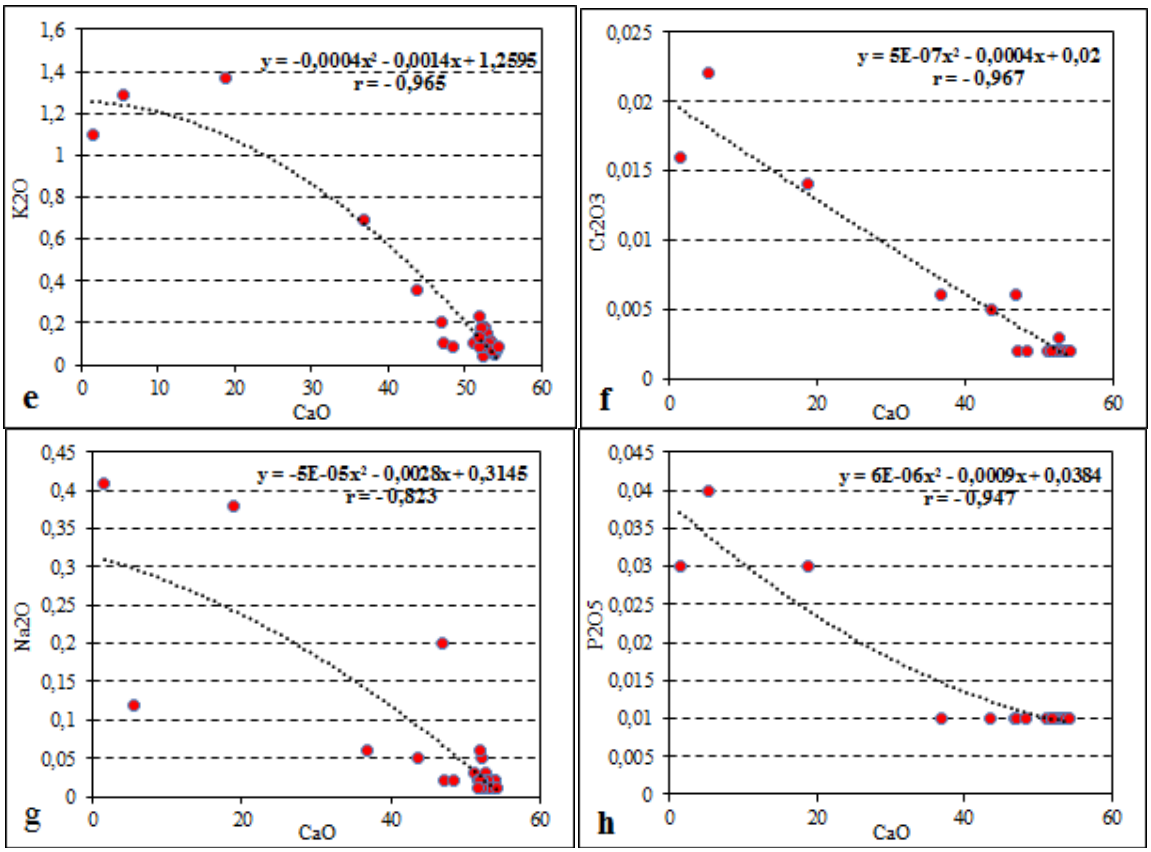

Fig. 18. Bivariate plots of the sample groups from the Kuşakdağı and Gökçepınar Formations a) CaO vs. SiO2, b) CaO vs. Al_2O_3, c) CaO vs. Fe_2O_3, d) CaO vs. TiO_2, e) CaO vs. K_2O, f) CaO vs. Cr_2O_3, g) CaO vs. Na_2O, h). CaO vs. P_2O_5.

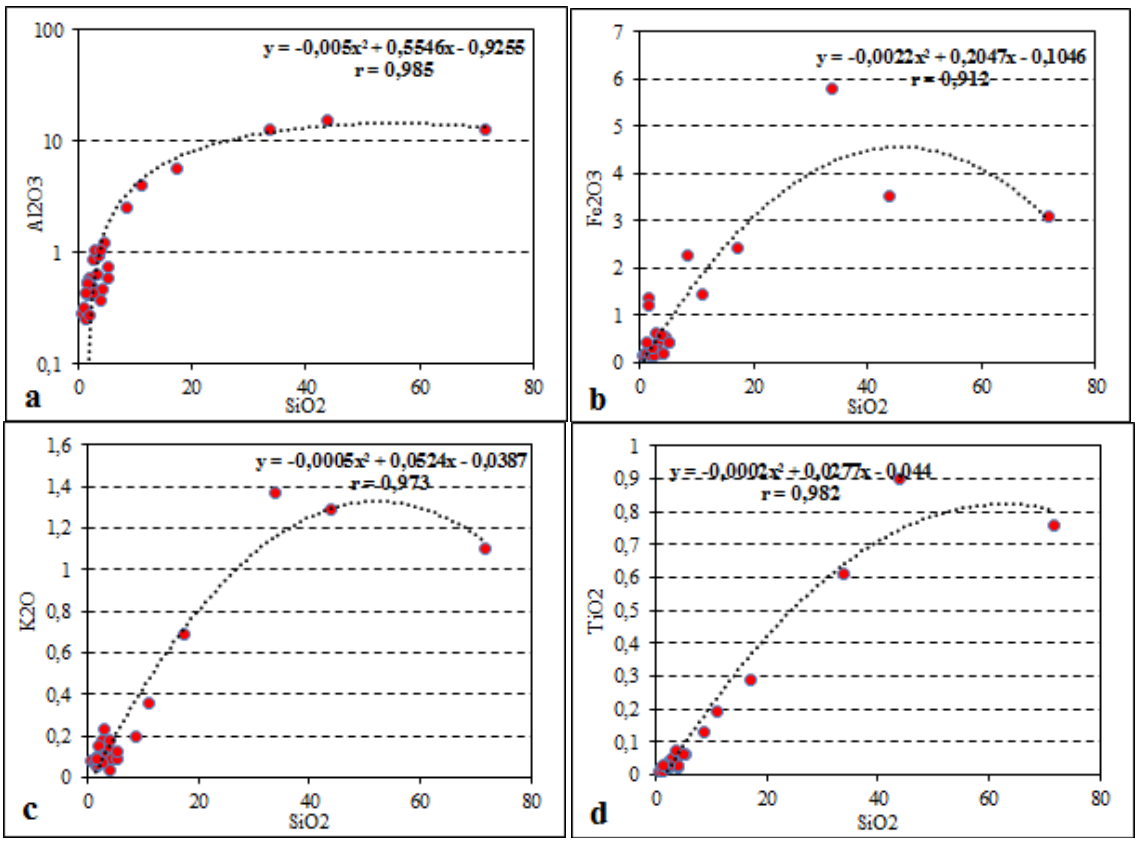

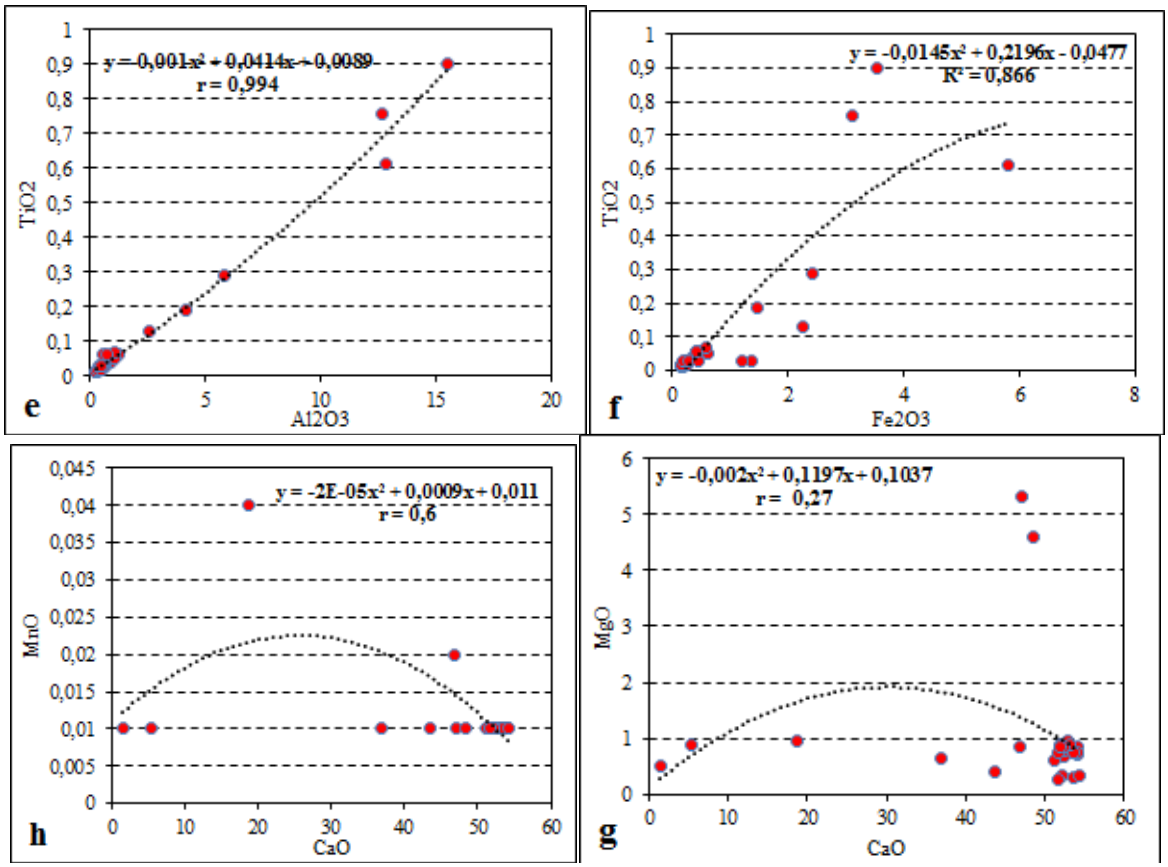

Fig. 19. Bivariate plots of the sample groups from the Kuşakdağı and Gökçepınar Formations. a) SiO_2 vs. Al_2O_3, b) SiO_2 vs. Fe_2O_3, c) SiO_2 vs. K_2O, d) SiO_2 vs. TiO_2, e) TiO_2 vs. Al_2O_3, f) TiO_2 vs. Fe_2O_3, g) CaO vs. MgO, h) CaO vs. MnO.

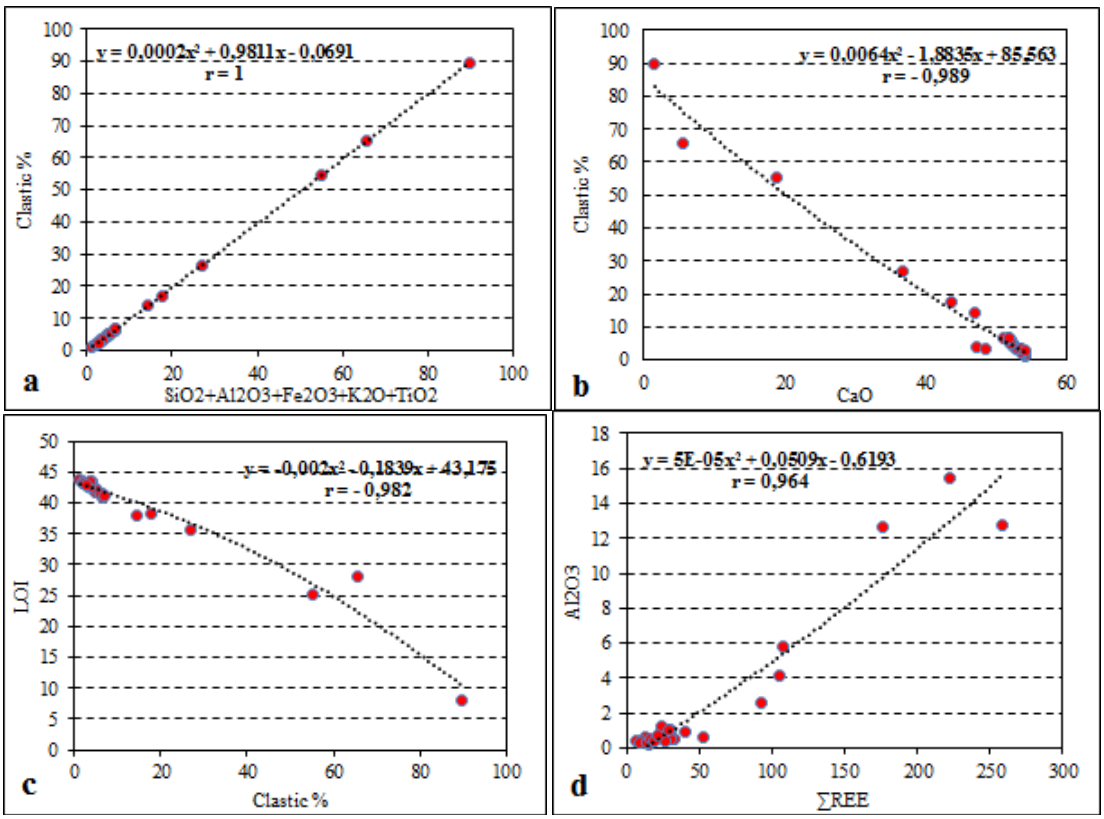

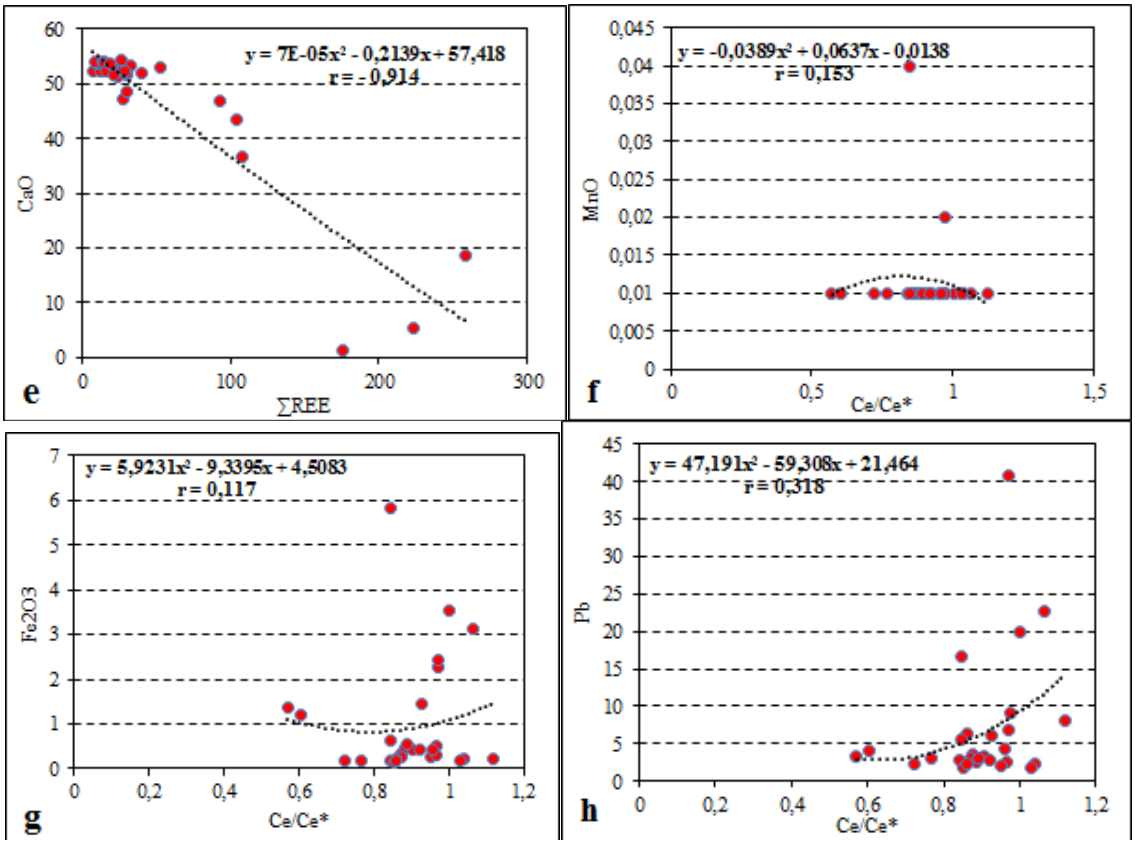

Fig. 20. Bivariate plots of the sample groups from the Kuşakdağı and Gökçepınar Formations. a) SiO_2+Al_2O_3+Fe_2O_3+Na_2O +K_2O+TiO_2 vs. Clastic %, b) CaO vs. Clastic%, c. LOI vs. Clastic%, d) ΣREE vs. Al_2O_3, e) ΣREE vs. CaO, f) Ce/Ce* vs. MnO, g) Ce/Ce* vs. Fe_2O_3, h) Ce/Ce* vs. Pb.

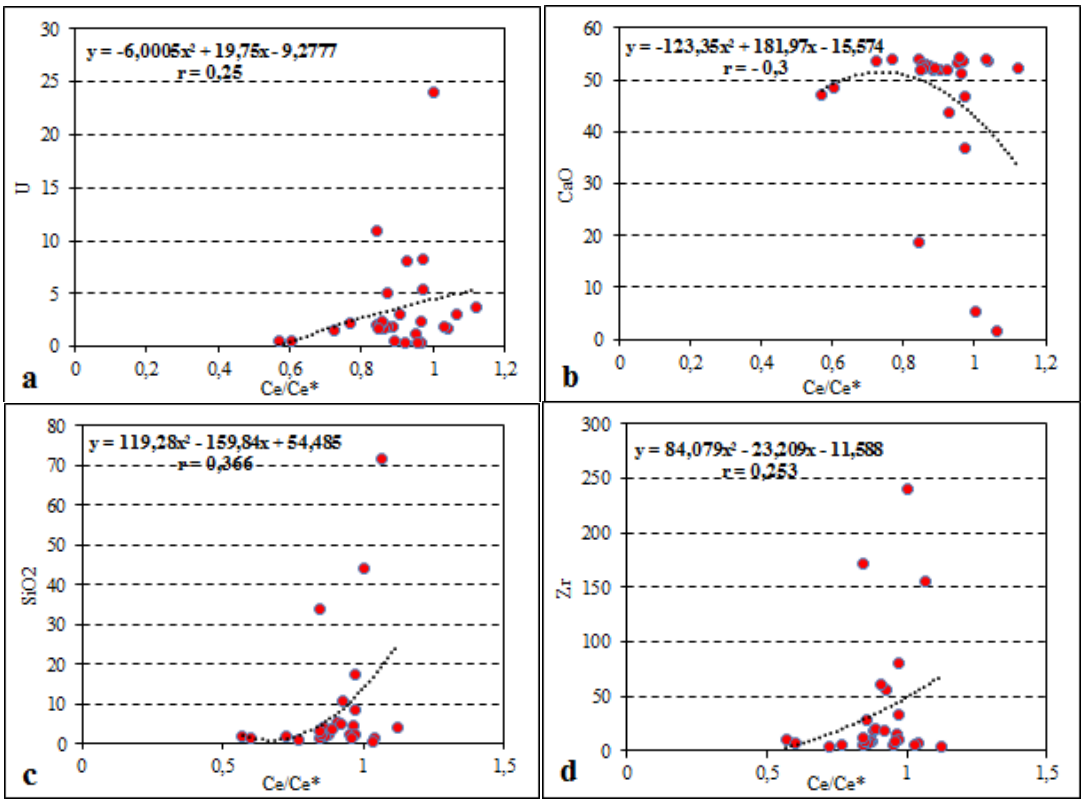

Fig. 21. Bivariate plots of the sample groups from the Kuşakdağı and Gökçepınar Formations. a) Ce/Ce* vs. U, b) Ce/Ce* vs. CaO, c) Ce/Ce* vs. SiO_2, d) Ce/Ce* vs. Zr.

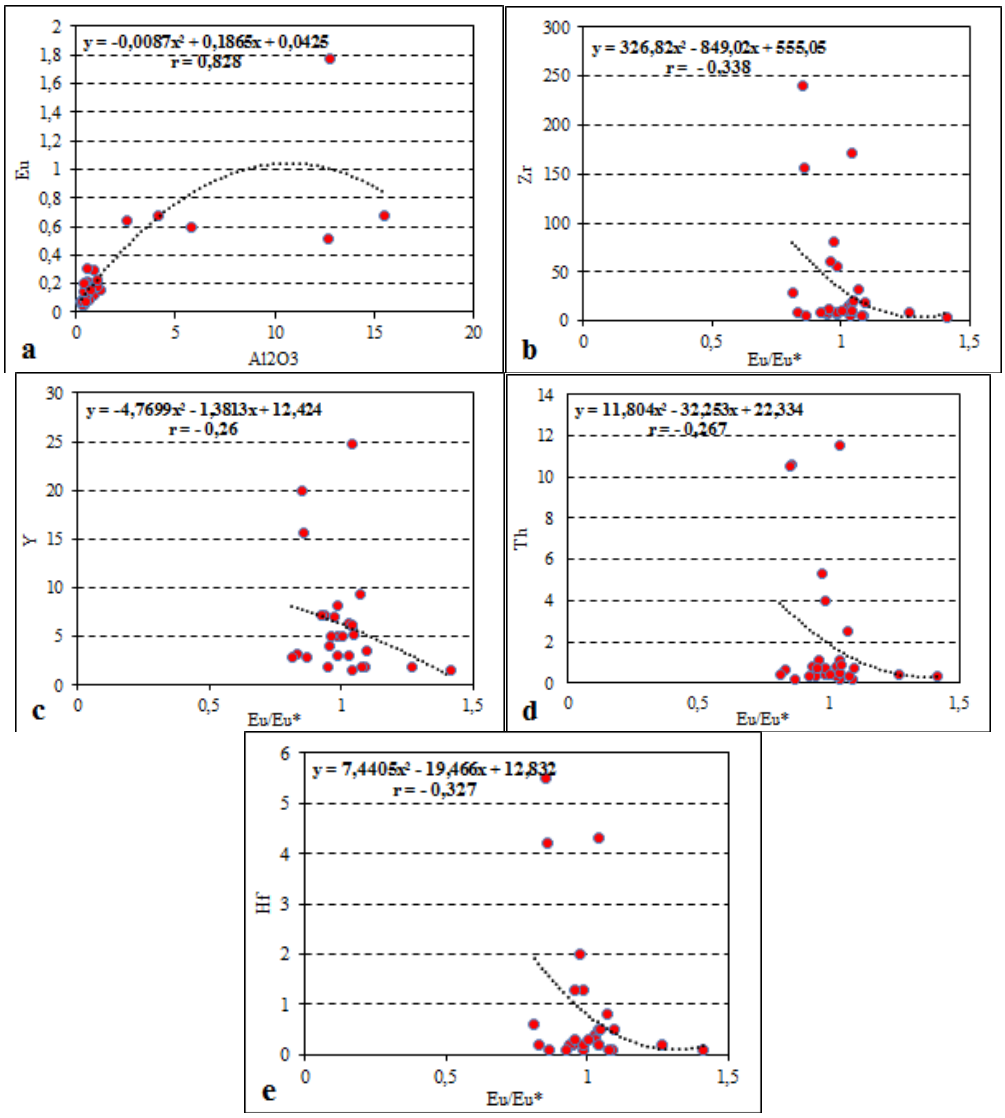

Fig. 22. Bivariate plots of the sample groups from the Kuşakdağı and Gökçepınar Formations. a) Eu vs. Al_2O_3, b) Eu/Eu* vs. Zr, c) Eu/Eu* vs. Y, d) Eu/Eu* vs. Th, e) Eu/Eu* vs. Hf.

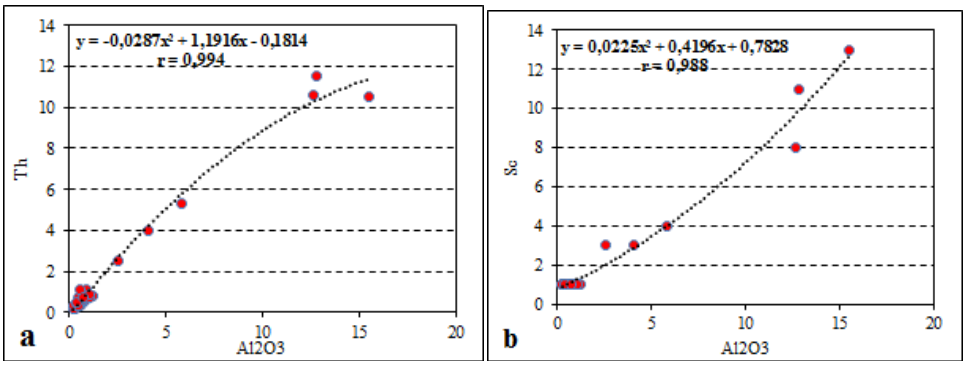

Fig. 23. Bivariate plots of the sample groups from the Kuşakdağı and Gökçepınar Formations. a) Al_2O_3 vs. Th, b) Al_2O_3 vs. Sc.

J. Kareem and Ş. Küpeli. "Trace Including Ree Y And Organic Geochemistry Of Kuşakdağı And Gökçepinar Formations In The Beyreli (Hadim-Konya) Area, Central Taurides, Southern Turkey: Implications For Source Rock Potential, Provenance, Paleo-Environment And Tectonic Setting." IOSR Journal of Applied Geology and Geophysics (IOSR-JAGG) 5.4 (2017): 06-35.